Research Paper

GEOSPHERE

GEOSPHERE, v. 20, no. 4

https://doi.org/10.1130/GES02748.1

20 figures; 2 tables; 1 set of supplemental files and 1 figure at full size

CORRESPONDENCE: greened@denison.edu

CITATION: Greene, D.C., Lackey, J.S., and Klemetti, E.W., 2024, Revised geologic map and structural interpretation of the Mineral King pendant, southern Sierra Nevada, California (USA): Evidence for kilometer-scale folding and structural imbrication of a Permian to mid-Cretaceous volcanosedimentary assemblage: Geosphere, v. 20, no. 4, p. 1190–1223, https://doi.org/10.1130/GES02748.1.

Science Editor: Christopher J. Spencer
Associate Editor: Terry L. Pavlis

Received 30 December 2023
Revision received 27 March 2024
Accepted 29 May 2024

Published online 10 July 2024

GOLD OPEN ACCESS

THE GEOLOGICAL SOCIETY OF AMERICA®

This paper is published under the terms of the CC-BY-NC license.

© 2024 The Authors

Revised geologic map and structural interpretation of the Mineral King pendant, southern Sierra Nevada, California (USA): Evidence for kilometer-scale folding and structural imbrication of a Permian to mid-Cretaceous volcanosedimentary assemblage

David C. Greene[1], Jade Star Lackey[2], and Erik W. Klemetti[1]

[1]Department of Earth and Environmental Sciences, Denison University, Granville, Ohio 43023, USA
[2]Geology Department, Pomona College, Claremont, California 91711, USA

ABSTRACT

The Mineral King pendant is an ~15-km-long, northwest-striking assemblage of Permian to mid-Cretaceous metavolcanic and metasedimentary rocks that form a steeply dipping wall-rock screen between large mid-Cretaceous plutons of the Sierra Nevada batholith (California, USA). Pendant rocks are generally well layered and characterized by northwest-striking, steeply dipping, layer-parallel cleavage and flattening foliation and steeply northwest-plunging stretching lineation. Northwest-elongate lithologic units with well-developed parallel layering and an absence of prominent faults or shear zones suggests a degree of stratigraphic continuity. However, U-Pb zircon dating of felsic metavolcanic and volcanosedimentary rocks across the pendant indicates a complex pattern of structurally interleaved units with ages ranging from 277 Ma to 101 Ma.

We utilize a compilation of 39 existing and new U-Pb zircon ages and four reported fossil localities to construct a revised geologic map of the Mineral King pendant that emphasizes age relationships rather than lithologic or stratigraphic correlations as in previous studies. We find that apparently coherent lithologic units are lensoidal and discontinuous and are cryptically interleaved at meter to kilometer scales. Along-strike facies changes and depositional unconformities combine with kilometer-scale tight folding and structural imbrication to create a complex map pattern with numerous discordant units.

Discrete faults or major shear zones are not readily apparent in the pendant, although such structures are necessary to produce the structural complications revealed by our new mapping and U-Pb dating. We interpret the Mineral King pendant to be structurally imbricated by a combination of kilometer-scale tight to isoclinal folding and cryptic faulting, accentuated by, and eventually obscured by, pervasive flattening and vertical stretching that preceded and accompanied emplacement of the bounding mid-Cretaceous plutons. Deformation in the Mineral King pendant represents a significant episode of pure-shear-dominated transpression between ca. 115 Ma and 98 Ma that adds to growing evidence for a major mid-Cretaceous transpressional orogenic event affecting the western U.S. Cordillera.

David Greene https://orcid.org/0000-0002-6384-9752

INTRODUCTION

Isolated wall-rock remnants exposed within the Sierra Nevada batholith (California, USA) provide a record of the late Paleozoic and Mesozoic Cordilleran continental margin that is otherwise largely obscured by subsequent intrusion of Jurassic and Cretaceous plutons (e.g., Saleeby et al., 1990; Schweickert and Lahren, 1991; Saleeby and Busby, 1993; Greene and Schweickert, 1995; Stevens and Greene, 1999, 2000; Tobisch et al., 2000; Memeti et al., 2010; Paterson and Memeti, 2014; Saleeby and Dunne, 2015; Cao et al., 2016; Barth et al., 2018; Attia et al., 2018, 2021; Clemens-Knott and Gevedon, 2023). These remnants of early arc rocks are preserved primarily as steeply dipping wall-rock screens (historically referred to as "roof pendants") between Cretaceous plutons.

The Mineral King pendant of this study is located in the central axial region of the southern part of the batholith (Fig. 1). The pendant is an ~15-km-long, northwest-striking assemblage of late Permian to mid-Cretaceous metavolcanic and metasedimentary rocks, exposed in a narrow belt between Cretaceous granitic plutons (Fig. 2). Strata are steeply dipping, tightly folded, and structurally interleaved, exposing a complex history of volcanic-dominated, predominantly shallow marine sedimentation in a continental margin magmatic arc setting. Rocks of the Mineral King pendant span the entire development of the Sierra Nevada magmatic arc, from its inception in the late Permian to mid-Cretaceous silicic volcanism essentially coeval with final emplacement of the Cretaceous batholith in this area at 99–98 Ma. The Mineral King pendant

Downloaded from http://pubs.geoscienceworld.org/gsa/geosphere/article-pdf/20/4/1190/6584248/ges02748.1.pdf
by guest

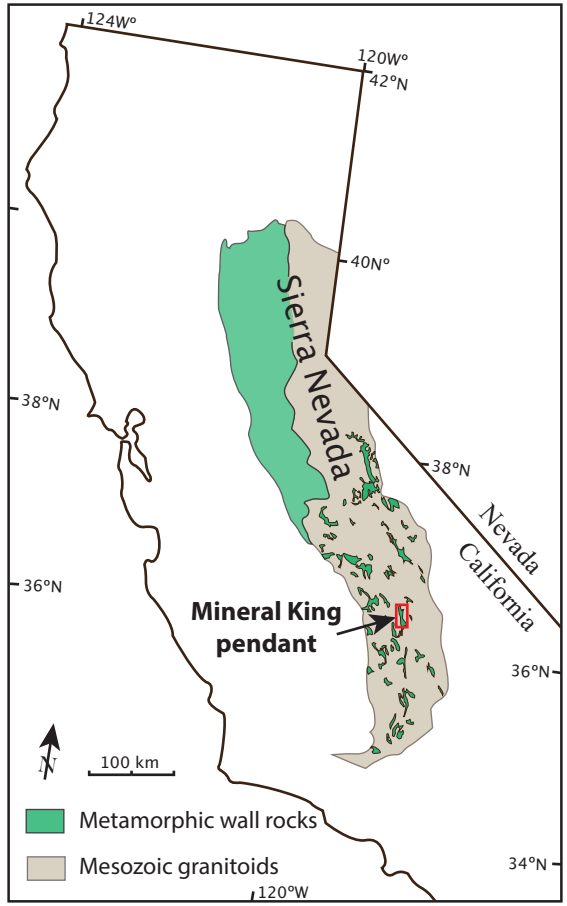

Figure 1. Location of the Mineral King pendant in the central axial region of the southern Sierra Nevada batholith, California, USA. Adapted from Jennings (1977).

Figure 2. Oblique aerial image of the Mineral King pendant, California, USA. View is north-northwest, centered on Farewell Canyon and the valley of the East Fork Kaweah River. Northwest-striking, steeply dipping metamorphic rocks of the Mineral King pendant form rusty orange and dark gray slopes on both sides of the valley. Late Paleozoic and Mesozoic pendant rocks are bounded to the east and west by mid-Cretaceous granitic plutons of the Sierra Nevada batholith, exposed in light gray cirques and ridges. Mineral King pendant as seen in this view is ~3 km wide and 15 km long. Image modified from Google Earth. Base image © 2024 Airbus.

does not, however, expose rocks of the Paleozoic "framework terranes," such as the Morrison block (Stevens and Greene, 1999; Greene and Stevens, 2002) and El Paso terrane (Dunne and Suczek, 1991; Clemens-Knott and Gevedon, 2023) upon which the Sierra Nevada magmatic arc was constructed.

Numerous studies have proposed large-scale strike-slip offset of the Cordilleran continental margin before and during emplacement of the Sierra Nevada batholith (e.g., Nokleberg, 1983; Kistler, 1990, 1993; Schweickert and Lahren, 1990, 1991, 1993; Saleeby and Busby, 1993; Greene et al., 1997; Tikoff and de Saint Blanquat, 1997; Wyld and Wright, 2001; Nadin and Saleeby, 2008; Memeti et al., 2010; Chapman et al., 2015; Clemens-Knott and Gevedon, 2023). These proposals have included major orogen-parallel shear zones, strike-slip ribbons, and intrabatholithic breaks of various types. Many of these proposed megascale structures are either older than the predominantly Late Cretaceous rocks of the Sierra Nevada batholith or cryptic and not well expressed in the granitic rocks. The Mineral King pendant is close to the trace of many

Downloaded from http://pubs.geoscienceworld.org/gsa/geosphere/article-pdf/20/4/1190/6584248/ges02748.1.pdf
by guest

of these proposed large-offset structures, and the stratigraphic affinity and structural history of the pendant can provide constraints on these proposed megascale structures.

Herein we present a compilation of 39 new and existing U-Pb zircon ages from Mineral King pendant rocks (Table 1). We utilize these age constraints along with known fossil occurrences (Table 2) and our new structural investigations to construct a revised geologic map of the Mineral King pendant (Fig. 3; full-size version of Fig. 3 is available online [link in caption]). Two new cross sections (Fig. 4) that emphasize age relationships, rather than lithologic (e.g., Sisson and Moore, 2013) or stratigraphic (e.g., Busby-Spera, 1983) correlations, are also presented. We find that the Mineral King pendant is structurally imbricated by a combination of kilometer-scale tight to isoclinal folding and cryptic faulting and is not an intact east-dipping homocline as some past interpretations have suggested. Pervasive flattening and vertical stretching of all pendant rocks preceded and accompanied emplacement of the bounding mid-Cretaceous plutons, indicating a major period of mid-Cretaceous transpressive deformation. We utilize these new results to discuss the stratigraphic and structural framework of the Mineral King pendant in the context of the southern Sierra Nevada.

PREVIOUS WORK

The Mineral King area was the focus of early prospecting and a short-lived mining boom in the 1870s, focused primarily on lead-zinc skarns associated with contact metamorphism of marble intruded by Cretaceous granitoid plutons (Goodyear, 1888; Goodwin, 1958; Sisson and Moore, 2013; Ryan-Davis et al., 2019). The area was first systematically mapped by Knopf and Thelan (1905). Unpublished mapping by John Dillon and students in 1969 (T. Sisson, 2011, personal commun.) included delineation of a major kilometer-scale synform on Vandever Mountain and smaller folds on Mineral Peak and in the area between Tulare Peak and Bullfrog Lakes previously identified by Christensen (1959, 1963).

Busby-Spera (1983) conducted detailed field mapping and stratigraphic investigations in the Mineral King pendant, with emphasis on the volcanic stratigraphy and the stratigraphic consequences of felsic volcanic eruptions in a marine environment (Busby-Spera, 1984, 1986). Busby-Spera (1983) produced a new geologic map of the pendant that emphasized stratigraphic and facies relationships especially within the volcanic units. Following then-current models for Sierran pendants (e.g., Bateman and Wahrhaftig, 1966; Fiske and Tobisch, 1978), Busby-Spera (Busby-Spera, 1983; Busby-Spera and Saleeby, 1987; Saleeby and Busby, 1993) concluded that the steeply dipping pendant strata constituted an overall east-facing homocline with only minor intraformational folding.

Subsequent investigation and mapping by Sisson and Moore (2013) favored map units defined by lithology and emphasized strike-parallel continuity of map units. Several single-grain U-Pb zircon ages suggested that the pendant stratigraphy does not in fact constitute an intact east-facing homocline but is instead complexly imbricated with numerous structural slices of late Paleozoic and Mesozoic age (Sisson and Moore, 2013).

DESCRIPTION OF THE DATA AND REVISED MAP

Revised Geologic Map

This study was originally conceived as an investigation of the structural geometry and deformation history of the Mineral King pendant, with the specific goal of identifying and characterizing major strike-slip faults proposed to transect the pendant and surrounding areas (e.g., Kistler, 1990, 1993; Schweickert and Lahren, 1991; Saleeby and Busby, 1993; Memeti et al., 2010; Chapman et al., 2015; Nadin et al., 2016). However, we have found no unambiguous strike-slip faults or discrete ductile shear zones of regional significance during this investigation. Instead, pendant rocks show evidence of distributed ductile flattening and primarily symmetric, pure shear vertical stretching (Christensen, 1963; Sisson and Moore, 2013; Van Auken and Greene, 2013; Worm and Greene, 2016).

Our new U-Pb zircon ages increasingly indicated that the volcanosedimentary stratigraphy contained far more discontinuities than originally envisioned (e.g., Klemetti et al., 2014; Hoffman et al., 2017; Greene et al., 2020), and these complexities were not adequately represented by existing geologic maps. The focus of the investigation therefore evolved from a dominantly structural study utilizing existing geologic mapping to the compilation of a revised geologic map based on a more extensive database of U-Pb zircon ages than had been available to previous workers. We concur with the majority of lithologic descriptions, map units, and unit boundaries of Sisson and Moore (2013), and thus we present our geologic map of the Mineral King pendant as a revision of the work of Sisson and Moore (2013) rather than as a new geologic map. Our revised map of the Mineral King pendant (Fig. 3) combines U-Pb zircon age data (Table 1) with Google Earth image interpretation and limited new field mapping and structural studies. In contrast to prior published mapping, we define and correlate map units based primarily on interpreted age rather than volcanosedimentary facies (Busby-Spera, 1983) or lithology (Sisson and Moore, 2013).

The locations of newly defined structural breaks and stratigraphic discontinuities are highlighted on our map by a revised color scheme that facilitates easier recognition of unit ages and relationships than was possible with previous published maps. This revised map is, however, a "work in progress", and substantial uncertainties still exist that will require further detailed mapping and dating to resolve.

U-Pb Zircon Dating

Over the course of this investigation, we collected and dated 23 samples using U-Pb zircon techniques, and these results are compiled and reported

Downloaded from http://pubs.geoscienceworld.org/gsa/geosphere/article-pdf/20/4/1190/6584248/ges02748.1.pdf
by guest

TABLE 1. U-Pb ZIRCON AGES FROM MINERAL KING PENDANT

Sample number	Map unit	Location		Age (Ma)	Source
		Lat (°N)	Long (°W)		
MK-1	Kmrt 3	36.3986	118.5752*	135.2 ± 5†	Busby-Spera (1983), Sisson and Moore (2013)
MK-520	Kmrt 1	36.4535	118.6059*	131.0 ± 4†	Busby-Spera (1983), Sisson and Moore (2013)
MK-530	Kmrt 2	36.4554	118.5887*	140.3 ± 6†	Busby-Spera (1983), Sisson and Moore (2013)
MK-540	Trma	36.4549	118.5852*	235.8 ± 6†	Busby-Spera (1983), Sisson and Moore (2013)
MK-822	Sill§ in Trss	36.4081	118.5656*	138.4 ± 4†	Busby-Spera (1983), Sisson and Moore (2013)
MK-900	Kmrt 2	36.4604	118.5909*	137.9 ± 4†	Busby-Spera (1983), Sisson and Moore (2013)
MK-910	Jmdt	36.4649	118.5907*	188.8 ± 5†	Busby-Spera (1983), Sisson and Moore (2013)
MK-920	Kma	36.4672	118.6036*	110.6 ± 3†	Busby-Spera (1983), Sisson and Moore (2013)
MK-980	Jslv	36.4717	118.5676*	170.9 ± 5†	Busby-Spera (1983), Sisson and Moore (2013)
MK-1700	Trvc	36.4395	118.5767*	214.2 ± 6†	Busby-Spera (1983), Sisson and Moore (2013)
08SMK035	Kwc	36.4233	118.6001	135.0 ± 1.0	Sisson and Moore (2013)
08SMK036	Dike§ in Jcsv	36.4239	118.6031	98.4 ± 0.5	Sisson and Moore (2013)
09SMK050	Kem	36.4692	118.5763	106.2 ± 1.1	Sisson and Moore (2013)
10JS03	Kmrt 1	36.4587	118.6068	136.5 ± 2.7	Klemetti et al. (2014)
11MK02	Kmrt 3	36.3988	118.5757	134.2 ± 0.7	Klemetti et al. (2014)
10JS05	Kmrt 2	36.4549	118.5897	135.5 ± 1.4	Klemetti et al. (2014)
10JS04	Jmdt	36.4653	118.5898	195.7 ± 1.4	Klemetti et al. (2014)
MD17	Kem	36.4659	118.5821	108.5 ± 1.0	D'Errico et al. (2012)
MK-105	Kma	36.4677	118.6035	104.7 ± 1.0	(This study–MSU)
MK-104	Porphyroclast§ in in Kmrt1	36.4665	118.6106	114.8 ± 3.1	(This study–MSU)
MK-17	Jslv	36.4673	118.5678	183.3 ± 2.0	(This study–MSU)
MK-31	Trvc	36.4383	118.5770	218.1 ± 2.5	(This study–MSU)
MK-179c	Kmt	36.4916	118.6013	118#	(This study–Stanford)
MK-173b	Kma	36.4677	118.6035	99.0 ± 2.0	(This study–Stanford)
MK-186	Kmrd	36.4293	118.6004	100.5 ± 0.9	(This study–Stanford)
MK-160b	Jcsv	36.4234	118.6028	183.8 ± 1.7	(This study–Pomona)
MK-204	Pvs	36.4290	118.5883	269#	(This study–Pomona)
MK-207	Jmdt	36.4743	118.5940	185.0 ± 2.3	(This study–Pomona)
MK-242	Jhb	36.4854	118.5564	182.5 ± 2.8	(This study–Pomona)
MK-259	Kvcs	36.4678	118.5741	135.6 ± 1.3	(This study–Pomona)
MK-264	Ksl	36.4730	118.5596	104.2 ± 1.4	(This study–Pomona)
MK-331	Jcsh	36.4499	118.5647	197.7 ± 1.0	(This study–Pomona)
MK-352	Kvcs	36.4441	118.5640	135.4 ± 1.0	(This study–Pomona)
MK-370	Trma	36.4514	118.5767	248.7 ± 1.1	(This study–Pomona)
MK-374	Pvt	36.4680	118.6081	276.9 ± 1.9	(This study–Pomona)
MK-376	Jgb	36.4525	118.5940	161.8 ± 1.7	(This study–Pomona)
MK-378	Kvcs	36.4032	118.5880	134.2 ± 1.0	(This study–Pomona)
MK-23	Trss	36.4065	118.5703	239#	Attia et al. (2021)
MK-318	Jvs	36.4323	118.6040	187#	Attia et al. (2021)

Notes: Sample coordinates are referenced to the World Geodetic System 1984 datum. Samples from this study indicate the laboratory where U-Pb geochronology was conducted (MSU—Michigan State University; Stanford—Stanford–U.S. Geological Survey Micro Analysis center; Pomona—Pomona College). Interpreted ages are weighted mean ^{207}Pb-corrected $^{206}Pb/^{238}U$ ages. Uncertainty of these ages reported at two standard deviations. Analytical methodology and results on unknowns and secondary standards are tabulated in File S1 (see text footnote 1). Plots used for interpretation of ages are also included in File S1.

*Busby-Spera (1983) sample location coordinates are pre-GPS and approximate. Published coordinates are reported here, but age locations plotted on map are adjusted to closest likely location based on outcrop.

†Date reported here is lower-intercept concordia age, recalculated by Sisson and Moore (2013) from original data of Busby-Spera (1983).

§Local intrusion; does not date the surrounding unit.

#Detrital zircon maximum depositional age.

Downloaded from http://pubs.geoscienceworld.org/gsa/geosphere/article-pdf/20/4/1190/6584248/ges02748.1.pdf
by guest

TABLE 2. TRIASSIC FOSSIL OCCURRENCES*

Source	Description
Busby-Spera (1983, 1984)	Late Triassic brachiopods along Crystal Creek from the first marble bed west of the thick metarhyolite tuff at ~2750 m (~9000 ft) in elevation
Busby-Spera and Saleeby (1987)	Late Triassic and possible Early Jurassic fossils north of Bullfrog Lakes
Turner (1894) and Durrell (1940)	Ammonites and pelecypod *Halobia* at 2750 m (9000 ft) elevation along Franklin Creek
Sisson and Moore (2013)	Pelecypod *Monotis* and indeterminate weakly deformed ammonites at 3200 m (10,480 ft) on the southwestern side of the small basin northwest of Tulare Peak
Christensen (1959)	Fossils including the ammonite *Clionites*, pelecypods *Halobia superba*, *Monotis*, and *Paleoneilo*, and brachiopod *Spiriferina* within narrow belts mainly of siliceous and calc-silicate hornfels along the east wall of the Mineral King and uppermost Little Kern valleys, from Crystal Creek south to Bullfrog Lakes
Smith (1927)	Reported *Pseudomonotis subcircularis* and *Paleoneilo* from Mineral King area but with no locations

*Primarily from Sisson and Moore (2013).

here (Table 1; Supplemental Material[1]). In addition, we incorporate previously reported U-Pb zircon dating of Busby-Spera (1983), D'Errico et al. (2012), Sisson and Moore (2013), Klemetti et al. (2014), and Attia et al. (2021) and reported fossil localities as compiled by Christensen (1963) and Sisson and Moore (2013). Dates are presented in tabular form in Table 1, and sample locations and preferred ages are indicated on the geologic map (Fig. 3).

Individual ages were determined using a variety of techniques with varying degrees of precision and uncertainty. Ambiguities and uncertainties for each age determination are discussed in the following sections and details of methodology and results can be found in the Supplemental Material. We include all age determinations on the geologic map and indicate a preferred age for each map unit.

U-Pb Zircon Ages of Busby-Spera (1983)

The originally reported ages of Busby-Spera (1983) were determined using multi-grain zircon splits and were ambiguous or in error due to incorporation of entrained older zircon grains. These ages were recalculated as lower-intercept concordia ages by Sisson and Moore (2013, their table 1), and those results are utilized herein. In general, these recalculated ages agree well with subsequent single-grain zircon ages. These samples were collected prior to the advent of GPS location, and thus their reported locations in grid coordinates have significant uncertainties and do not always fall in the outcrop area of the units they represent. Grid locations as tabulated in Sisson and Moore (2013, their table 1) are also reported in our Table 1. However, plotted map locations for these samples have been adjusted to indicate the most likely location of each sample based on access and exposure of the relevant unit.

[1]Supplemental Material. Includes analytical methodology and plots used for interpretation of ages. Please visit https://doi.org/10.1130/GEOS.S.26008276 to access the supplemental material, and contact editing@geosociety.org with any questions.

U-Pb Zircon Age of D'Errico et al. (2012)

D'Errico et al. (2012) utilized a sensitive high-resolution ion microprobe–reverse geometry (SHRIMP-RG) to date zircons from the quartz diorite of Empire Mountain (map unit Kem) that yielded a weighted mean $^{206}Pb/^{235}U$ age of 108.5 ± 1.0 Ma in the course of an investigation of its emplacement history.

U-Pb Zircon Ages of Sisson and Moore (2013)

Sisson and Moore (2013) utilized the SHRIMP-RG at the Stanford–U.S. Geological Survey (USGS) Micro Analysis Center (Stanford, California) to date four Cretaceous plutons in and adjacent to the Mineral King pendant. These include the deformed granodiorite of White Chief Mine (map unit Kwc), the quartz diorite of Empire Mountain (Kem), and the very large plutons that bound the Mineral King pendant to the west (granodiorite of Castle Creek, Kcc) and to the east (granite of Coyote Pass, Kcp). Sisson and Moore (2013) also dated a deformed felsite dike of mid-Cretaceous age that intrudes pendant rocks near Eagle Lake.

U-Pb Zircon Ages of Klemetti et al. (2014)

Klemetti et al. (2014) utilized the SHRIMP-RG at the Stanford-USGS Micro Analysis Center to perform 51 spot analyses on zircons from four metavolcanic units within the pendant, which yielded ages of ca. 135 Ma for three rhyolite tuff units (map units Kmrt1, Kmrt2, and Kmrt3) and an age of 196 Ma for a dacitic tuff (Jmdt) (Table 1).

U-Pb Detrital Zircon Ages of Attia et al. (2021)

U-Pb geochronology analyses of zircons from two Mineral King samples were conducted by laser ablation–inductively coupled plasma–mass

Downloaded from http://pubs.geoscienceworld.org/gsa/geosphere/article-pdf/20/4/1190/6584248/ges02748.1.pdf
by guest

Geologic Map of Mineral King Pendant, Sequoia National Park, California

Revised from Sisson and Moore (2013)

GEOLOGIC UNITS

QUATERNARY

Q — **Surficial deposits** – unconsolidated surficial deposits, undivided.

MIDDLE CRETACEOUS

Kap — **Aplite** – Fine-grained, very light colored aplitic granite with conspicuous blue-black tourmaline.

Kcc — **Granodiorite of Castle Creek** – Medium-grained hornblende-biotite granodiorite with prominent grains of hornblende and titanite. *U/Pb ages 98±2 Ma(a), 98±1 Ma(b), 98±1 Ma(c).*

Kcciz — **Injection zone along margin of granodiorite of Castle Creek** – Steeply dipping sheets of fine-grained granodiorite, 1 – 3 m thick, closely interleaved with metamorphic rocks along eastern contact with granodiorite of Castle Creek (Kcc).

Kmcp — **Diorite associated with granite of Coyote Pass** – Fine- and medium-grained hornblende diorite and quartz diorite intrusive into granite of Coyote Pass (Kcp); commonly includes angular granite blocks.

Kcp — **Equigranular facies of granite of Coyote Pass** – Light colored, medium- to coarse-grained biotite-hornblende granite. *U/Pb ages 97±2 Ma(a), 99±1 Ma(b)*

Kf — **Felsite** – fine-grained, very light colored granite; exposed at outlet of lower Franklin Lake.

Kmrd — **Felsic metavolcanic rocks** – Metarhyolite tuff, fine- to medium-grained volcanogenic sandstone, and mixed metadacite tuffs and flows, E side Miners Ridge. *U/Pb age 107±1 Ma(d)*

Ksl — **Granodiorite of Spring Lake** – Medium to fine-grained granodiorite with sparse mafic dikes; possibly lighter colored facies of quartz diorite of Empire Mountain. *U/Pb age 104±1 Ma(d)*

Kma — **Meta-andesite** – Metamorphosed andesitic lava flows, breccias and interleaved felsic metavolcanic rocks west of Timber Gap. *U/Pb ages 111±1 Ma(a), 105±1 Ma(d), 99±2 Ma(d)*

Kem — **Quartz diorite of Empire Mountain** – Medium-grained quartz diorite cut by sparse mafic dikes; *U/Pb ages 107±1 Ma(a), 106±1 Ma(b), 109±1 Ma (Dirrico et al., 2012).*

Kmt — **Metarhyolite tuffs and sandstone** – variably reworked felsic volcanic tuffs, breccias and quartzofeldspathic sandstone, Cliff Creek area. *U/Pb dr age ≤118 Ma (d)*

EARLY CRETACEOUS

Kvbr — **Metarhyolite and metadacite breccia** – Lenses and beds of felsic volcanic breccia with relict angular clasts, Vandever Mountain.

Kmrt3 — **Metarhyolite Tuff** – Massive metarhyolite with relic pyroclastic texture; includes some interstratified quartzofelspathic sandstone and volcanic breccia; Vandever Mtn. *U/Pb ages 135±5 Ma(a), 134±1 Ma(c)*

Kcgl — **Calc-silicate conglomerate** – Dark weathering, well-bedded calc-silicate conglomerate and pebbly sandstone with white felsite clasts. Underlies Kmrt3 in synclinorium on north ridge of Vandever Mountain.

Kwc — **Granodiorite of White Chief Mine** – Sheared, medium-grained hornblende-biotite granodiorite with well-developed foliation, sheared and offset mafic and aplitic dikes. *U/Pb age 135±1 Ma(b)*

Kvcs — **Felsic volcanic and volcaniclastic sedimentary rocks** – Rhyolite and dacite tuffs, some with pyroclastic texture; variably reworked to biotite quartzofeldspathic sandstone and interlayered with calc-silicate hornfels and volcanic breccia. Interpreted correlative units at Bullion Flat, and north of Cold Spring. *U/Pb ages of 136±1 Ma(d) east side of Empire Mountain, 135±1 Ma(d) south side of Mineral Peak, 134±1 Ma(d) west side of Vandever Mountain.*

Kmrt2 — **Metarhyolite tuff** – Massive metarhyolite with relic pyroclastic texture; includes some interstratified quartzofelspathic sandstone and volcanic breccia; east of Timber Gap. *U/Pb ages 140±6 Ma(a), 138±4(a), 136±1 Ma(c)*

Kmrt1 — **Metarhyolite Tuff** – Massive metarhyolite with relic pyroclastic texture; includes some interstratified quartzofelspathic sandstone and volcanic breccia; north of Cold Spring. *U/Pb ages 131±4 Ma(a), 137±3 Ma(c)*

JURASSIC

Jgb — **Hornblende gabbro** – Medium- to coarse-grained hornblende gabbro, intrusive sill on east side of Mineral King valley. Interpreted correlative unit on southwest side of Empire Mountain. *U/Pb age 162±2 Ma(d).*

Jhb — **Hornblende gabbro** – Medium- to coarse-grained hornblende gabbro and diorite; Black Rock Pass. *U/Pb age 183±3 Ma(d)*

Jslv — **Metadacite tuff and tuff breccia** – Interlayered biotite-plagioclase dacite tuff and tuff breccia, some variably reworked to quartzofeldspathic sandstone. Cut by a distinctive series of white felsite dikes. Interpreted as a possible caldera fill sequence. Exposed west of Spring Lake. *U/Pb ages 171±5 Ma(a), 183±2 Ma(d)*

Jcsv — **Calcsilicate and felsic volcanic rocks** – Thinly bedded calcareous quartzite interlayered with quartzofeldspathic sandstone, variably reworked felsic tuffs, and volcanic breccias; Eagle Lake area. *U/Pb age 184±2 Ma(d)*

Jmdt — **Metadacite tuff** – Massive metadacite tuff with relict pyroclastic texture. Distinguished from metarhyolite tuffs (Kmrt) by more abundant biotite and hornblende and absence of relict quartz phenocrysts; west side of Empire Mountain. *U/Pb ages 189±5 Ma(a), 196±1 Ma(c), 185±2 Ma(d)*

Jvs — **Felsic volcaniclastic sedimentary rocks** – Biotite quartzofeldspathic sandstone and conglomerate with volcanic clasts, reworked felsic tuff, and some calcsilicate hornfels and marble; Miners Ridge. *U/Pb dr age ≤187 Ma(e)*

Jtc — **Tactite** – Dark brown, coarse-grained rocks consisting of calcic garnet, epidote, diopside, and idocrase developed along contacts between quartz diorite of Empire Mountain (Kem) and marble or calc-silicate rocks.

Jch — **Siliceous calc-hornfels** – Primarily thin-bedded, calcareous and calcsilicate hornfels, with interlayered felsic volcanic rocks. Some prominent marble layers present locally, and calcareous skarn alteration prominent near contacts with quartz diorite of Empire Mountain. Distinguished from calcsiliceous hornfels (Jcsh) by preponderance of calcareous rocks including marble.

Jcsh — **Calc-siliceous hornfels** – Orange weathering, thin-bedded, fine-grained, calc-silicate hornfels derived from calcareous quartzofeldspathic siltstone and sandstone; interbedded with gray-weathering, variably reworked, felsic tuffs and breccias. Distinguished from Jch by dominantly siliceous rocks and lack of prominent marble layers. *U/Pb age 198±1 Ma(d)*

MIDDLE TO LATE TRIASSIC

Trvc — **Felsic volcanic rocks and calc-silicate hornfels** – rhyolite tuffs and breccia interlayered with fine-grained, thin-bedded calcsilicate hornfels derived from calcareous quartzofeldspathic siltstone and sandstone. *U/Pb ages 214±6 Ma(a), 218±3 Ma(d)*

Trm — **Marble** – Coarsely crystalline white to blue-gray marble, with thinly interbedded calc-silicate layers that locally constitute up to 50% of unit. *Late Triassic fossil localities(a,b)*

Trsc — **Siliceous and calc-silicate hornfels** – Predominantly orange-weathering, thin-bedded, fine-grained siliceous and calc-silicate hornfels derived from quartzo-feldspathic siltstone and sandstone. Subordinate interstratified meta-argillite and marble. *Late Triassic fossil localities(b)*

Trsa — **Siliceous hornfels** – Predominantly dark gray-weathering, thin-bedded, fine-grained siliceous hornfels with subordinate interstratified meta-argillite and marble. *Late Triassic fossil localities(b)*

Trss — **Metasandstone** – Well-bedded arkosic metasandstones, interpreted to be deposited by turbidity currents. Exposed primarily on Tulare Peak. *U/Pb dr age ≤239 Ma(e)*

Trma — **Meta-andesite** – Metamorphosed andesitic lava flows and breccias west of Mineral Peak. *U/Pb ages 236±6 Ma(a), 249±1 Ma(d)*

LATE PERMIAN

Psp — **Slate and phyllite** – Predominantly dark gray-weathering, fissile slate, phyllite, and dark colored argillaceous hornfels derived from mudstone.

Pvs — **Volcaniclastic metasandstone** – Medium- to thin-bedded, medium- to coarse-grained lithic metasandstone, rare interstratified lenses of volcaniclastic breccia. Contains relict detrital grains of felsite and phenocrysts. *U/Pb dr age ≤269 Ma (d)*

Pvt — **Rhyolite tuff and siliceous hornfels** – Well-bedded, fine-grained siliceous and calc-siliceous hornfels with interlayered rhyolite tuff; north of Cold Spring. *U/Pb age 277±2 Ma(d)*

Lithologic descriptions modified in part from Sisson and Moore (2013).

Sources of ages identified by subscript: (a) Busby-Spera (1983), recalculated by Sisson and Moore (2013); (b) Sisson and Moore (2013); (c) Klemetti et al. (2014); (d) this study; (e) Attia et al. (2021). All ages are U/Pb zircon, dr indicates ages derived from detrital zircons. Preferred age indicated in red. Details for each age determination are provided in Supplemental Material. Locations of dated samples and preferred age are indicated on map.

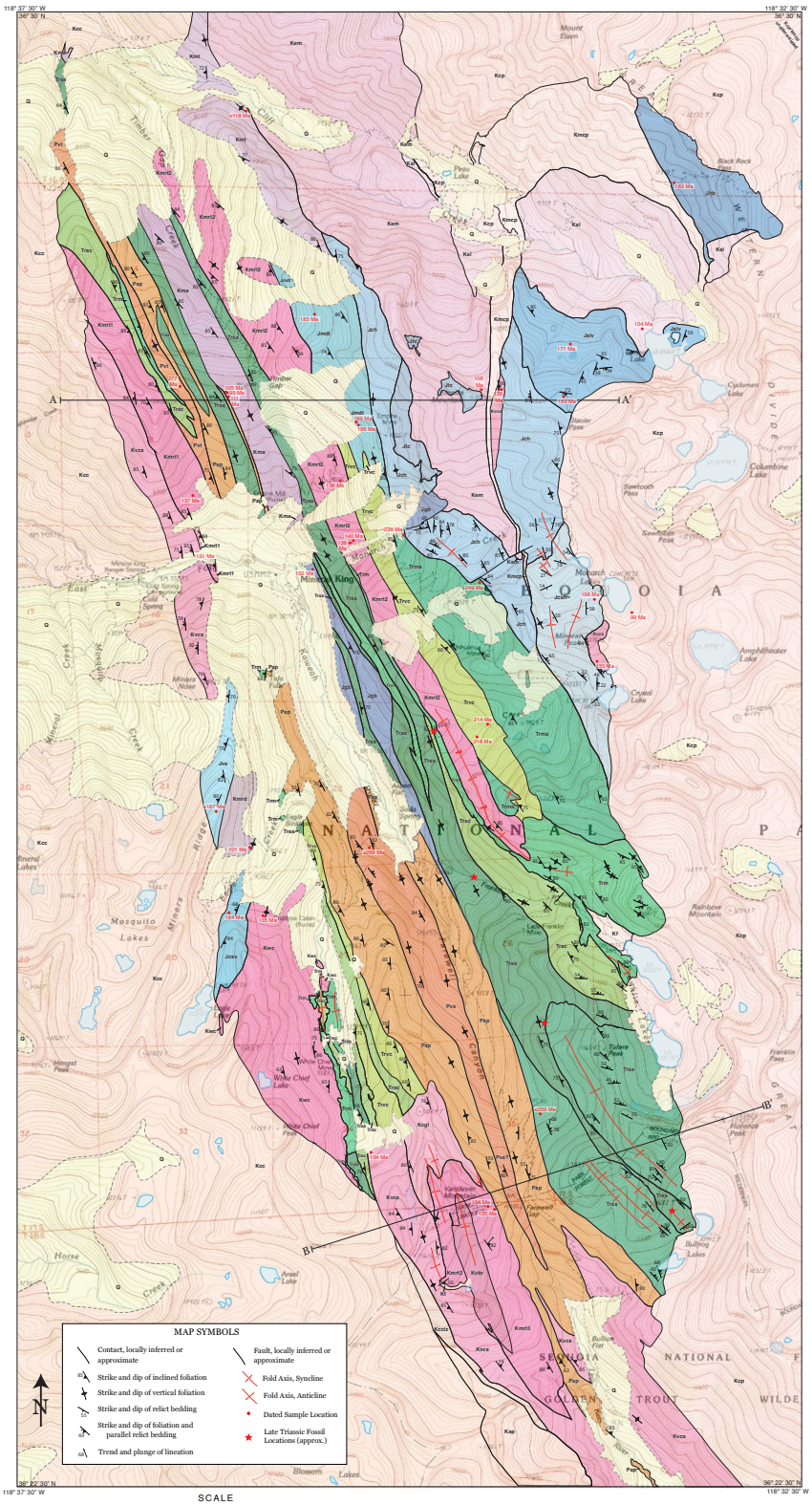

Figure 3. Revised geologic map of the Mineral King pendant, California, USA. Modified from Sisson and Moore (2013). To view Figure 3 at full size, please visit https://doi.org/10.1130/GEOS.S.26107945 or access the full-text article on www.gsapubs.org.

Downloaded from http://pubs.geoscienceworld.org/gsa/geosphere/article-pdf/20/4/1190/6584248/ges02748.1.pdf
by guest

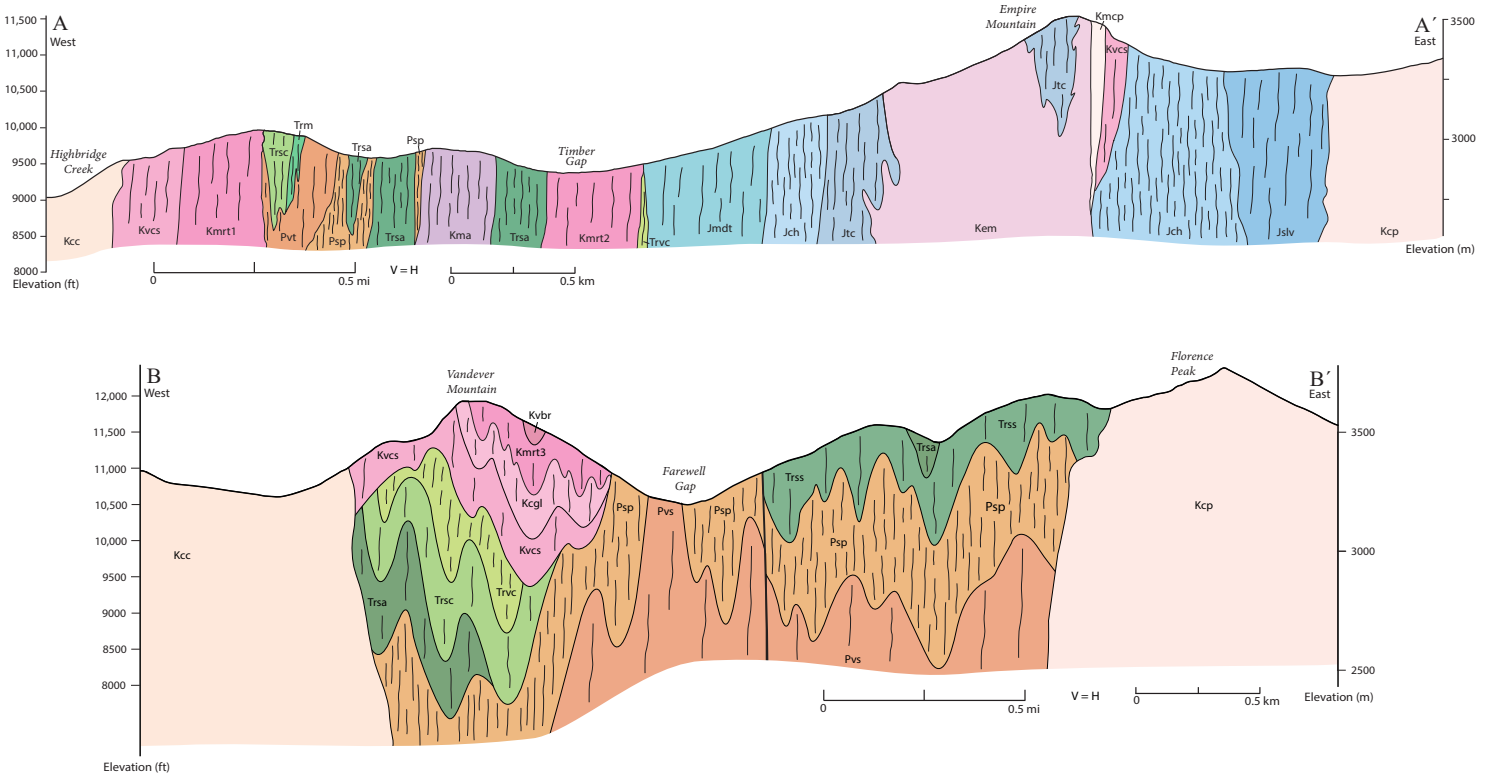

Figure 4. Cross sections of the Mineral King pendant, California, USA. Quaternary surficial deposits are omitted. Thin, wavy lines indicate approximate orientation of foliation. See geologic map (Fig. 3) for locations and geologic unit descriptions.

spectrometry (LA-ICP-MS) at the Arizona LaserChron Center (Tucson, Arizona, USA) (Attia et al., 2021). A sample of medium-grained volcaniclastic sandstone (map unit Trss) interpreted by Busby-Spera (1985) as turbidity current strata yielded a few Mesozoic grains with a spread of older ages (Attia et al., 2021). Maximum depositional ages for detrital zircon sample sets are normally determined from the youngest coherent group of three grains rather than from the single youngest age (Geherels, 2014), and by this standard the sample would be considered late Permian in age. However, two zircon grains in this sample yielded concordant ages of ca. 240 Ma, suggesting that the actual depositional age is likely Early Triassic, and the unit is therefore interpreted as Early Triassic in this study. A sample of volcanogenic sandstone from the western edge of the pendant on Miners Ridge yielded a major age peak at ca. 187 Ma with a spread of older Precambrian detrital ages (Attia et al., 2021).

New U-Pb Zircon Ages (This Study)

Nineteen new samples were dated in support of this study. This includes 16 samples dated by LA-ICP-MS at Michigan State University (East Lansing, Michigan, USA; $n = 4$) and Pomona College (Claremont, California; $n = 12$) and three samples dated using the SHRIMP-RG at the Stanford-USGS Micro Analysis Center. Details of analytical methodologies and isotope ratios of unknown and secondary standards and interpretation of ages are available in File S1 (see footnote 1). The interpreted ages from these new geochronology efforts are summarized in Table 1 but with notable patterns in the age distribution and "gaps" in age that are discussed below in Stratigraphy of the Mineral King Pendant section.

Among all newly dated samples, we note distinct regularity of recycling of zircon in magmas in the pendant. Such recycling is in the form of inherited

Downloaded from http://pubs.geoscienceworld.org/gsa/geosphere/article-pdf/20/4/1190/6584248/ges02748.1.pdf
by guest

zircons as old as 1.6 Ga (see File S1) but more commonly as more proximal episodes of magmatic activity. For example, one sample from map unit Kmt yielded ages from five concordant grains of 118 Ma, 120 Ma, 139 Ma, 182 Ma, and 190 Ma. We interpret these as detrital zircons from a reworked felsic volcaniclastic unit and 118 Ma as the approximate maximum depositional age of this unit. Recycling is commonly more cryptic in the form of discordance of $^{207}Pb/^{235}Pb$ and $^{206}Pb/^{238}U$ age of zircon grains. Such discordant analyses were typically excluded from interpretation of age unless, in the absence of concordant grains, their ^{207}Pb-corrected $^{206}Pb/^{238}U$ age was considered robust and mean squared weighted deviation (MSWD) values of a group of grains population were <2.0 (see File S1). Such discordance was clearly a cause of uncertainty of U-Pb age in early work by Busby-Spera on these rocks (Busby-Spera, 1983) and affects laser ablation analyses even with screening of zircon samples optically by cathodoluminescence. Some samples are notably "clean" without significant discordance, including more mafic lithologies such as the axial gabbro (unit Jgb) which was found to have a Middle Jurassic age of 161.8 ± 1.7 Ma.

The new ages document the oldest ages yet found in the Mineral King pendant including from Permo-Triassic interbeds in the clastic sequence: unit Pvt, 276.9 ± 1.9 Ma, and unit Trma, 248.7 ± 1.1 Ma. A maximum depositional age of 269 Ma is obtained for unit Pvs as well. Also evident is an active magmatic history in the Early Jurassic with multiple additional new dates falling between 182 and 185 Ma: 183.3 ± 2.0 Ma (Jslv), 183.8 ± 1.7 Ma (Jcsv), 185.0 ± 2.3 Ma (Jmdt), and 182.5 ± 2.8 Ma (Jhb), with additional dates in the interval of 197–201 Ma that are consistent with findings of similar ages in the Triassic to Early Jurassic.

Other patterns among our new ages include multiple Early Cretaceous volcanic interbeds of 134–135 Ma (map unit Kvcs). A sample of dacite tuff (Kmrd) from the west side of the pendant yielded an age of 100.5 ± 0.9 Ma, and rhyolite tuff samples from a thin interbed west of Timber Gap (Kma) yielded ages of 110.6 ± 3 Ma, 104.7 ± 1.0 Ma, and 99 ± 2 Ma. These dates on surface-deposited volcanic rocks within the pendant are notable for being very close to the dates of the bounding granitic plutons (98 Ma and 99 Ma), which were emplaced at 10.5–10.9 km depth (Klemetti et al., 2013).

STRATIGRAPHY OF THE MINERAL KING PENDANT

Mineral King pendant strata are metamorphosed to greenschist or lower amphibolite facies (Sisson and Moore, 2013), tilted to steep dips, and variably deformed. Premetamorphic protoliths are distinguishable in most cases, but tight folding and bedding transposition at all scales makes stratigraphic and facies analyses uncertain.

Metasedimentary rocks predominate in the pendant and include volcaniclastic metasandstones, calcareous and siliceous hornfels, slates, and argillites (Fig. 5). Marble is present locally, both as large mappable bodies (map unit Trm) and as lenses and interbeds within fine-grained siliceous and calc-siliceous units. Sedimentary protoliths were deposited primarily in shallow nearshore to offshore shelf environments, with some well-bedded sandstones interpreted as turbidites deposited in a submarine fan environment (Busby-Spera, 1985; Sisson and Moore, 2013). Most sedimentary units contain at least some volcanic-derived grains.

Metavolcanic rocks include massive metarhyolite tuffs, metadacite tuffs, and meta-andesite flows and breccias (Fig. 6). Metavolcanic rocks are commonly reworked, and apparent primary volcanic deposits interfinger with and grade laterally into volcaniclastic sedimentary units.

In general, stratigraphic units in the Mineral King pendant are not distinguishable based on lithology alone. Along-strike facies variations are common, for example, from primary volcanic rocks to reworked volcaniclastic sedimentary units. Thus, map units based primarily on lithology can change more-or-less arbitrarily along strike, as noted by Sisson and Moore (2013). Variably reworked felsic volcanic and volcaniclastic rocks, in particular, are typical lithologies across the entire span of pendant ages from late Permian to mid-Cretaceous. For example, similar-appearing thin-bedded calc-silicate hornfels and quartzofeldspathic sandstone with interlayered felsic tuffs have yielded ages ranging from 277 Ma (north of Cold Spring) to 198 Ma (west of upper Monarch Lake) to 184 Ma (north of Eagle Lake) to 136 Ma (east of Empire Mountain) to 105 Ma (west of Timber Gap).

Some distinctive units are present in the pendant, for example, the massive rhyolite tuffs of 134–137 Ma age (Kmrt1–Kmrt3) and the thin-bedded volcaniclastic sandstone on Tulare Peak (Trss) that has yielded a 239 Ma detrital zircon age (Attia et al., 2021). But in most of the Mineral King pendant, lithologic correlation is notably unreliable, and all units must be dated for accurate definition.

Our revised geologic map (Fig. 3) and accompanying cross sections (Fig. 4) group units of similar age based on our U-Pb dating results, allowing stratigraphic and structural assemblages to be more clearly delineated. Mapping by age relationships allows us to divide Mineral King strata into five tectonostratigraphic assemblages (Fig. 7). These assemblages are separated by four age gaps that correspond to important stratigraphic and structural discontinuities. Further dating may well narrow or eliminate some of these age gaps or more tightly constrain these episodic components to the development of the volcanic arc.

In the following sections, we describe the tectonostratigraphic assemblages and age gaps in chronological order from Permian through Cretaceous. The five mapped tectonostratigraphic assemblages are not necessarily coherent stratigraphic packages. In particular, the stratigraphic position of undated units within these assemblages should be considered speculative, as should the age and assemblage designation of any undated unit. Locations referred to in the text are indicated on Figure 8.

Late Permian Assemblage

Rocks of late Permian age are exposed in a northwest-trending, 0.2–1.2-km-wide band that runs the length of the Mineral King pendant. Rocks of this

Downloaded from http://pubs.geoscienceworld.org/gsa/geosphere/article-pdf/20/4/1190/6584248/ges02748.1.pdf
by guest

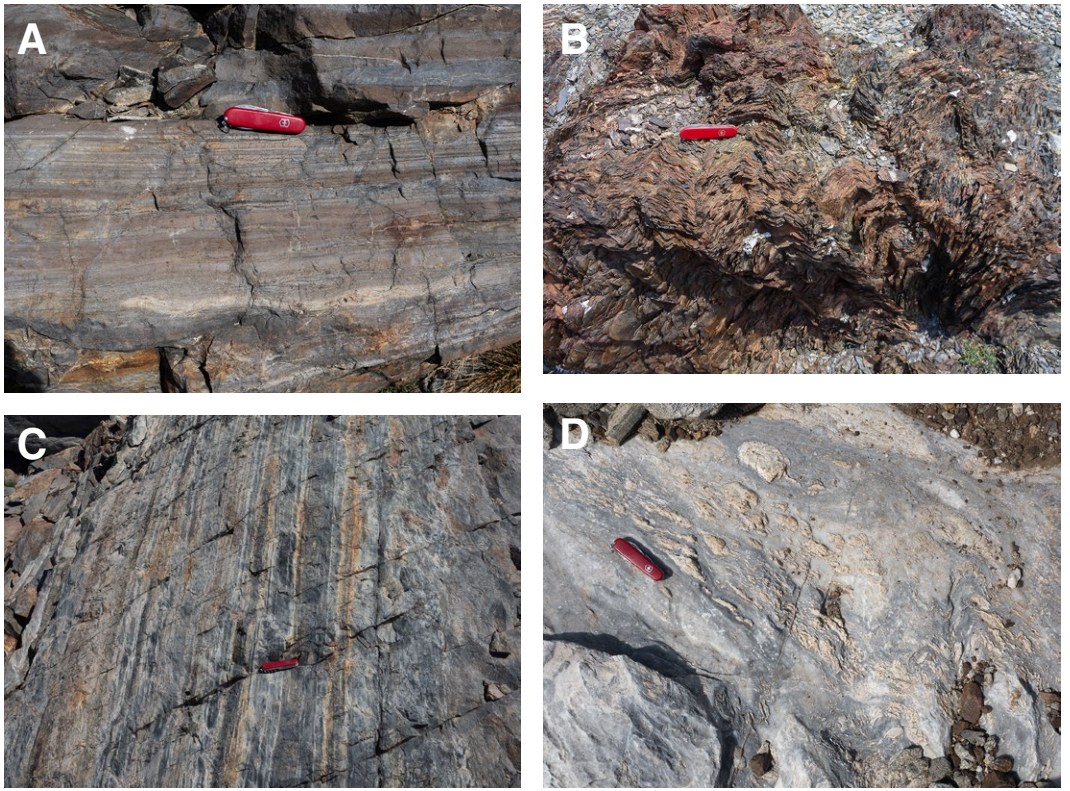

Figure 5. Representative metasedimentary rocks of the Mineral King pendant, California, USA. (A) Quartzofeldspathic metasandstone, interpreted as primarily reworked felsic volcanic ash. Characteristically well-bedded, finely laminated in part, with layering locally attenuated and discontinuous (36.4499°N, 118.5647°W). (B) Highly cleaved black siliceous argillite. Unit Psp near Farewell Gap (36.3993°N, 118.5719°W). (C) Well-layered, very fine-grained, calc-silicate hornfels derived from calcareous quartz siltstone. Unit Jch in upper Spring Lake cirque north of Glacier Pass (36.4668°N, 118.5713°W). (D) Gray and white, coarse-grained marble with deformed calc-silicate layers. Unit Trm near White Chief Mine (36.4087°N, 118.5910°W). Jackknife is 9 cm in length.

assemblage are well exposed at Farewell Gap and in Farewell Canyon as well as on the ridge west of Timber Gap. This assemblage is indicated in shades of orange on the geologic map (Fig. 3) and accompanying cross sections (Fig. 4).

The late Permian assemblage consists of three map units. The oldest unit of this assemblage (Pvt) is also the oldest dated unit in the Mineral King pendant, comprising well-bedded siliceous and calc-siliceous hornfels with interlayered rhyolite tuff. Exposed on the ridge west of Timber Gap, the rhyolite tuff has yielded an age of 276.9 ± 1.9 Ma. To the west, this unit appears to be interleaved with marble and calc-silicate hornfels of presumed Triassic age and to be truncated by an angular unconformity at the base of the Cretaceous rhyolite tuffs (Kmrt2).

A locally well-layered lithic metasandstone unit (Pvs) is exposed on the western side of Farewell Canyon and is interpreted to extend southward to a pinch-out south of Farewell Gap. This unit contains interstratified lenses of volcaniclastic breccia as well as relict detrital grains of felsite and phenocrysts (Sisson and Moore, 2013). A detrital zircon maximum depositional age of 269 Ma (based on a small population of six grains) was obtained from a pebbly, coarse-grained, volcaniclastic metasandstone layer in this unit west of Soda Spring. Top-direction indicators in this unit, predominantly thin graded beds and interlayer truncations, yield conflicting top directions on a meter scale that we interpret to indicate isoclinal folding and bedding transposition.

The third unit in this assemblage (Psp) consists of fine-grained, dark gray, fissile slate and phyllite (Fig. 5B) and dark-colored argillaceous hornfels and is broadly exposed on both the western and eastern sides of Farewell Canyon. Highly fissile, vertically dipping phyllite forms a narrow, easily weathered, strike-parallel slot canyon that constrains the East Fork Kaweah River as it flows northward from Farewell Gap. This unit is undated, but we interpret it as Permian based on its dominantly sedimentary character and close association with dated Permian units. The unit is interpreted to continue northward through a zone of no exposure to the ridge west of Timber Gap, where it is in contact with a 1-km-long lens of meta-andesite (Trma) of presumed Triassic age.

Downloaded from http://pubs.geoscienceworld.org/gsa/geosphere/article-pdf/20/4/1190/6584248/ges02748.1.pdf
by guest

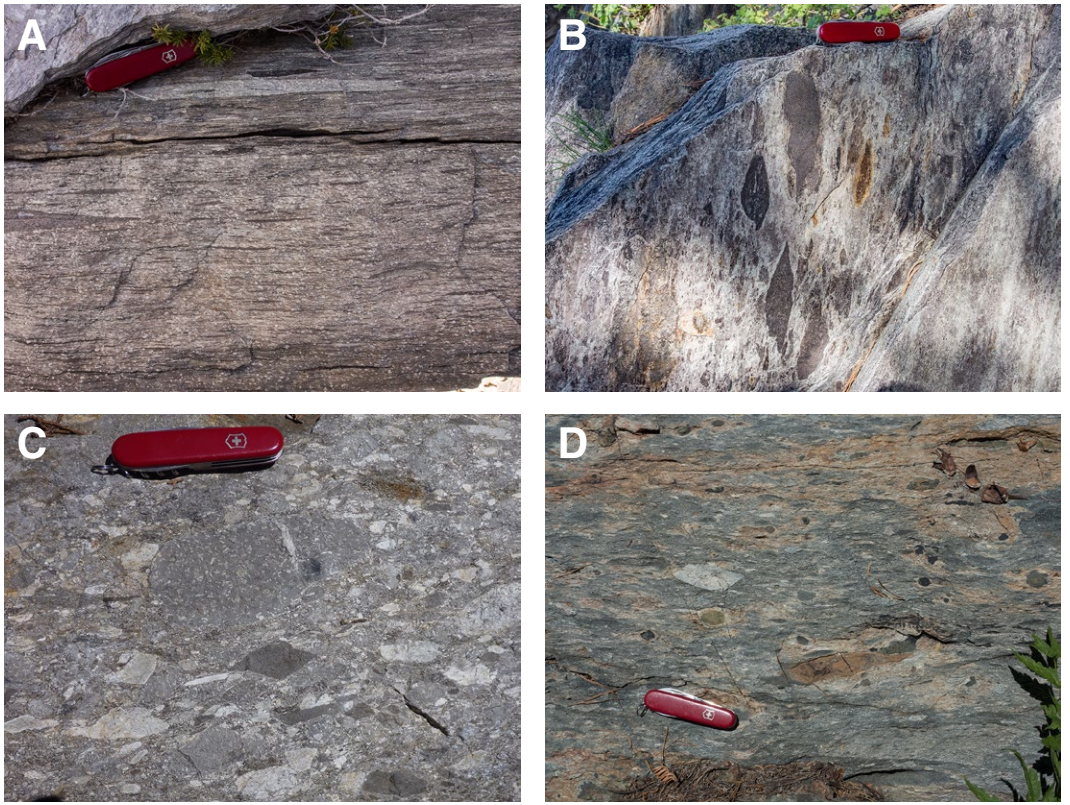

Figure 6. Representative metavolcanic rocks of the Mineral King pendant, California, USA. (A) Metarhyolite tuff with relict pyroclastic texture. Dark flattened pumice clasts and small, light-colored quartz and feldspar phenocrysts are characteristic. Image shows a horizontal surface, perpendicular to foliation and lineation. Unit Kmrt1 north of Cold Spring (36.4678°N, 118.6129°W). (B) Metarhyolite tuff showing dark, flattened pumice clasts and down-dip extension lineation. Image shows a vertical surface, parallel to foliation and lineation. Unit Kmrt1 north of Cold Spring, same location as A. (C) Heterolithologic volcanic breccia. Unit Trvc south of Monarch Creek (36.4530°N, 118.5870°W). (D) Reworked, epidote-altered volcanic breccia. Unit Kmt south of Cliff Creek (36.4822°N, 118.5971°W). Jackknife is 9 cm in length.

Age Gap 1

About 21 m.y. between the late Permian and Middle to Late Triassic assemblages is missing as indicated by our dating. Units of the Middle to Late Triassic assemblage bound the Permian assemblage on the eastern (and locally western) sides. Mapped contacts between these two assemblages are highlighted with a blue toothed line on Figures 8 and 9. On the eastern side of Farewell Canyon, the contact is parallel to the older Permian strata but truncates folded Middle Triassic units and interleaved Jurassic gabbro (Jgb), indicating at least localized faulting. A similar although less clearly developed relationship is expressed west of Farewell Canyon on the ridge north of Vandever Mountain. On the ridge west of Timber Gap in the northern pendant, the map pattern suggests tight folding and possible fault imbrication of Triassic strata into the Permian units.

We interpret this discontinuity to represent a late Permian unconformity that has localized subsequent (Triassic) thrust(?) faulting. Other pendants in the Sierra Nevada also exhibit a regional late Permian unconformity, apparently related to late Permian transpressive tectonism (e.g., Stevens et al., 2005; Saleeby and Dunne, 2015; Attia et al., 2018, 2021; Clemens-Knott and Gevedon, 2023). This unconformity is complicated in the Mineral King pendant by faulting and structural repetition of Triassic rocks.

Middle to Late Triassic Assemblage

Rocks of Middle to Late Triassic age are widely exposed in the southeastern area of the pendant and in a narrower band on the western side of the pendant in contact with granodiorite and rhyolite tuffs of the Early Cretaceous assemblage. Five Triassic U-Pb zircon ages have been obtained from strata within the pendant, and these along with reported Late Triassic fossil localities define the Triassic assemblage. The six discrete units of the assemblage are indicated by shades of green on the geologic map (Fig. 3) and accompanying cross sections (Fig. 4).

Downloaded from http://pubs.geoscienceworld.org/gsa/geosphere/article-pdf/20/4/1190/6584248/ges02748.1.pdf
by guest

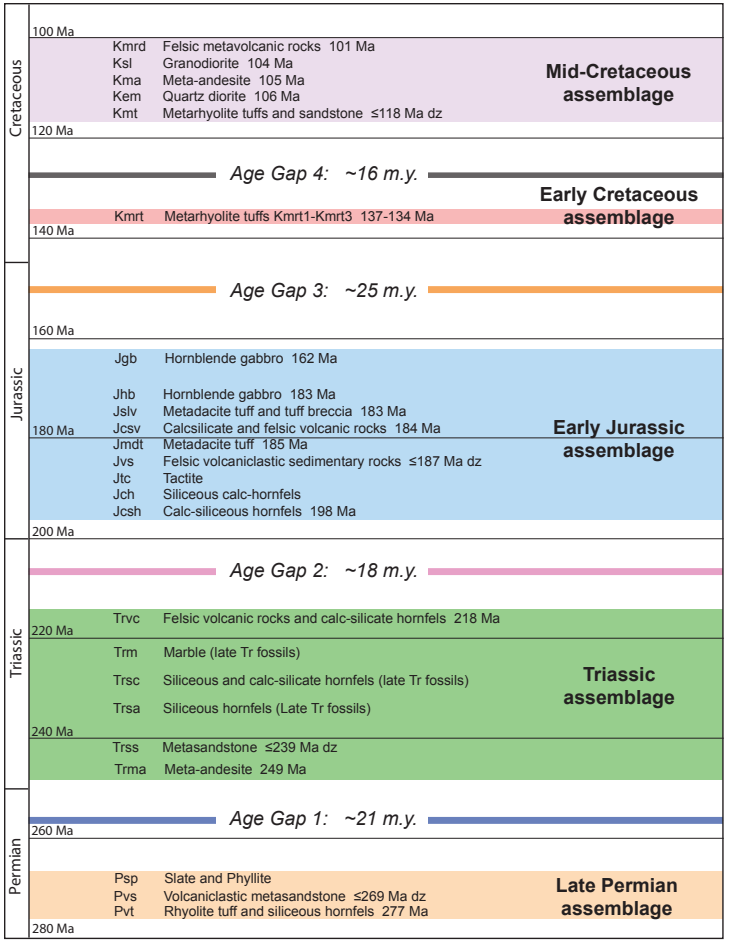

Figure 7. Tectonostratigraphic assemblages in the Mineral King pendant, California, USA, based on current U-Pb dating. Assemblages are defined based on clustering of ages and are not necessarily coherent stratigraphic packages. Age and assemblage designation of undated units are speculative. Age gaps between assemblages correspond to stratigraphic and structural discontinuities as discussed in the text, although further dating may more tightly constrain or even eliminate some of the age gaps indicated here. dz—detrital zircon age; Tr—Triassic.

The Triassic assemblage consists of meta-andesite, arkosic metasandstone, siliceous and calc-silicate hornfels, marble, and felsic volcanic rocks interbedded with calc-silicate hornfels and quartzofeldspathic siltstone. This assemblage is broadly lithologically similar to the overlying Jurassic assemblage, with massive Triassic marble being the exception. Further dating may reduce the apparent hiatus (age gap 2) and indicate that these two assemblages should be merged.

The oldest Triassic unit (Trma) is a thick meta-andesite exposed west of Mineral Peak and in the upper Crystal Creek drainage. A felsic volcanic layer near the eastern edge of this unit yielded a U-Pb zircon age of 248.7 ± 1.1 Ma, and a sample from the Monarch Creek drainage was dated at 236 ± 6 Ma (Busby-Spera, 1983; recalculated by Sisson and Moore, 2013).

Well-bedded, medium-grained, arkosic metasandstone (Trss) is widely exposed on the summit and flanks of Tulare Peak. This unit has a more distinctly sedimentary character than most units in the pendant and is interpreted to have been deposited by turbidity currents in a submarine fan (Busby-Spera and Saleeby, 1987; Sisson and Moore, 2013). Well-developed graded beds and small channel truncations indicate local depositional top directions, but these indicators conflict across outcrops at the meter to 10 m scale. Tight to isoclinal folds at 10 m to 100 m scale are visible in mountain-side exposures. We consider bedding in this unit to be entirely transposed. A sample from this metasandstone has yielded a suite of detrital zircon grains with a calculated maximum depositional age of 265 Ma (Attia et al., 2021). However, two younger grains yielded ages of 239 ± 3 Ma and 240 ± 3 Ma, suggesting that the actual age of deposition was Middle Triassic, and we interpret this Middle Triassic age to be most representative of the unit.

Units consisting of dark gray, thin-bedded siliceous hornfels (Trsa), orange-weathering, thin-bedded siliceous and calc-siliceous hornfels (Trsc), and coarsely crystalline white to blue-gray marble (Trm; Fig. 5D) are well exposed north of Tulare Peak and in the Franklin Creek drainage. Poorly preserved Late Triassic fossils have been reported from these units at a number of locations along the eastern side of Mineral King valley, including sites on Crystal Creek in unit Trm, on Franklin Creek in unit Trsc, and from the Bullfrog Lakes area in unit Trsa. These localities are summarized in Christensen (1963), Busby-Spera and Saleeby (1987), and Sisson and Moore (2013).

In addition to the mapped exposures of coarsely crystalline marble (Trm) and interbedded calc-silicates, numerous discontinuous lenses and stringers of white to blue-gray marble showing evidence of tight folding and ductile deformation are interlayered within the sedimentary protoliths of the Triassic assemblage; these are not separately indicated on the geologic map. Units in White Chief valley on the western side of the pendant are undated but interpreted as Triassic based on lithologic resemblance to fossiliferous Triassic units, especially in the presence of massive to thick-bedded blue-gray marble likely correlative to Trm (Fig. 5D).

The youngest dated Triassic unit (Trvc) is a rhyolite tuff interlayered with siliceous and calc-silicate hornfels and exposed in the Crystal Creek drainage. This unit has yielded ages of 218 ± 3 Ma (this study) and 214 ± 6 Ma (Busby-Spera, 1983; recalculated by Sisson and Moore, 2013).

Age Gap 2

There is an apparent age gap of ~18 m.y. between Late Triassic felsic volcanic and calc-silicate strata (map units Trvc, Trsc, and Trm) exposed in the

Downloaded from http://pubs.geoscienceworld.org/gsa/geosphere/article-pdf/20/4/1190/6584248/ges02748.1.pdf
by guest

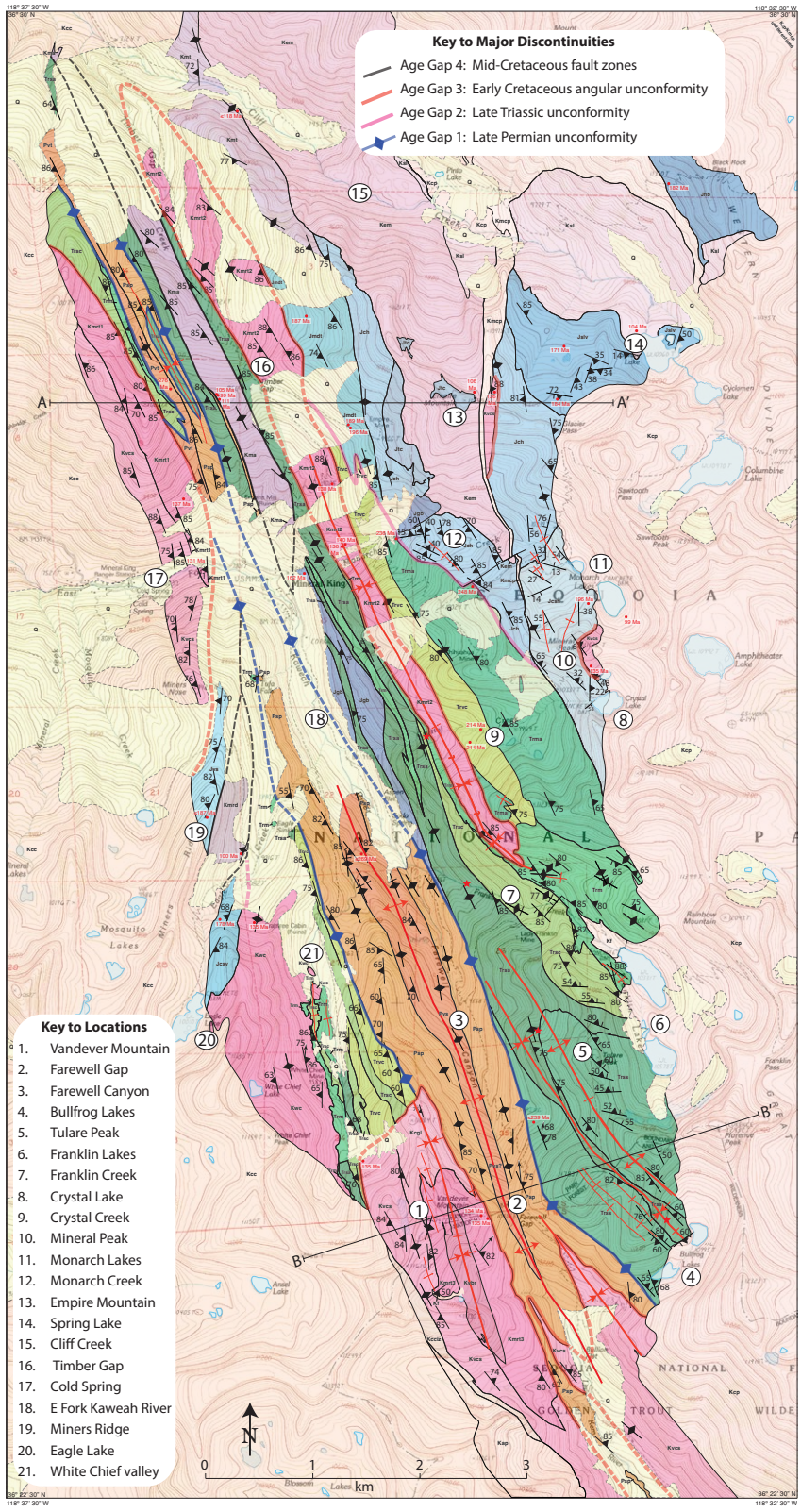

Figure 8. Interpretive version of geologic map (Fig. 3) and key to locations referred to in text. Figure is drawn to emphasize the contacts between tectonostratigraphic assemblages that we interpret to be major discontinuities. Structures indicated are speculative, and we consider it likely that most of the discontinuities indicated here have a significant component of ductile shearing. In our interpretation, the northern pendant is dominated by tectonically imbricated fault slivers of diverse ages (Fig. 9A), whereas the structural pattern in the southern pendant is dominated by kilometer-scale northwest-trending folds (Fig. 9B). See Figure 3 for map units and symbols.

Downloaded from http://pubs.geoscienceworld.org/gsa/geosphere/article-pdf/20/4/1190/6584248/ges02748.1.pdf
by guest

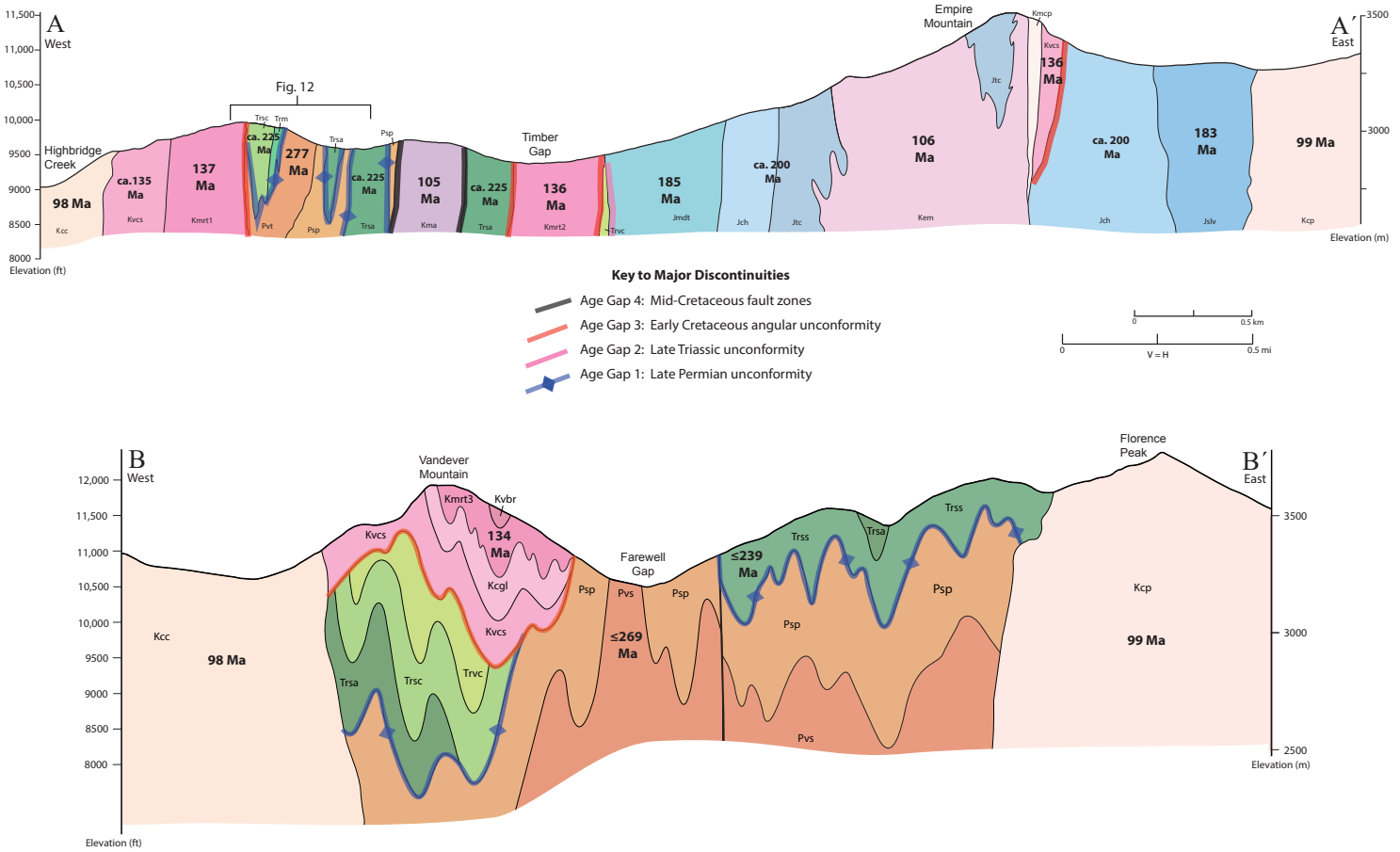

Figure 9. Interpretive cross sections emphasizing major discontinuities. Quaternary surficial deposits are omitted. See Figure 8 for locations and Figure 3 for geologic unit descriptions. (A) Section across the northern pendant along the line A-A′, illustrating the contrasts in ages between adjacent units. Map units are directly dated by U-Pb in zircon, except those indicated as circa (ca.) which are dated via correlation with units to the south and have a much higher degree of uncertainty. Diverse ages of units in sharp contact across variably deformed vertical boundaries suggest a complex pattern of tectonically imbricated fault slivers. See also Figure 12 for an annotated photograph of a portion of this section. (B) Section across the southern pendant along the line B-B′, illustrating speculative interpretation of a continuous, northwest-trending fold train resulting from mid-Cretaceous contractional deformation.

Crystal Creek drainage and Early Jurassic siliceous and calc-siliceous hornfels (Jcsh and Jch) on the northeastern edge of the pendant. Contacts between these assemblages are shown in pink on Figures 8 and 9.

The Triassic assemblage is lithologically similar to the overlying Jurassic assemblage, and units with Late Triassic fossils could be as young as the base of the Jurassic assemblage. Further dating may thus reduce the apparent hiatus and indicate that these two assemblages should be merged.

There is, however, a substantial discontinuity between the Triassic and Jurassic assemblages on the eastern side of the pendant in the Monarch Creek and Crystal Creek drainages. In this locality, Triassic meta-andesite (Trma) dated at 249 Ma is in contact with the Jurassic calc-siliceous hornfels unit (Jcsh) dated at 198 Ma. Regionally, this time period corresponds to the development of a proposed Late Triassic carbonate platform that is represented by deformed Late Triassic marbles in many of the southern Sierra Nevada pendants (Saleeby

Downloaded from http://pubs.geoscienceworld.org/gsa/geosphere/article-pdf/20/4/1190/6584248/ges02748.1.pdf
by guest

and Dunne, 2015; Attia et al., 2021). The deformed Late Triassic marble unit (Trm) at Mineral King is likely a remnant of this regional carbonate platform, and thus a significant unconformity would be expected at this time based on regional considerations.

Early Jurassic Assemblage

The Early Jurassic assemblage is exposed mostly on the eastern side of the pendant, on both the eastern and western flanks of Empire Mountain. Units of this assemblage are indicated by shades of blue on the geologic map (Fig. 3) and accompanying cross sections (Fig. 4).

The Early Jurassic assemblage consists of (1) siliceous, calc-siliceous, and calcareous hornfels (units Jch and Jcsh) and variable tactite skarn (Jtc); (2) a massive dacite tuff unit exposed on the western side of Empire Mountain (Jmdt); and (3) a distinctive unit of metadacite tuff and tuff breccia exposed west of Spring Lake (Jslv). In addition, two isolated slivers of Early Jurassic rocks (Jvs and Jcsv) are present on the western edge of the pendant north of Eagle Lake with unclear relationship to the main body of the assemblage. The assemblage is intruded by hornblende gabbro bodies (Jgb and Jhb) of Early and Middle Jurassic age. Nine Early Jurassic ages have been obtained from pendant rocks, ranging from 197.7 ± 1.0 Ma to 183.3 ± 2.0 Ma.

Type 1 units (as described in the previous paragraph) are more calcareous than other units of the assemblage. The calc-siliceous hornfels unit (Jcsh; Fig. 5A) is exposed in the cirques west of Monarch and Crystal Lakes on the eastern edge of the pendant. This unit is characterized by distinctive, orange-weathering, thin-bedded, quartzofeldspathic metasiltstone interbedded with felsic tuffs and has yielded a date of 197.7 ± 1.0 Ma on a felsic tuff layer. Unit Jcsh lies east of a ductile shear zone that separates it from the bulk of the pendant to the west. Folding is more open in this area, and bedding generally has more moderate dips than in other areas of the pendant.

The siliceous calc-hornfels unit (Jch; Fig. 5C) is similar to Jcsh except that calcareous hornfels and marble are more prominent components. This unit is split and wedged apart by intrusion of the Cretaceous quartz diorite of Empire Mountain (Kem), which appears to have intruded as a southward-thinning, steeply dipping sill. The siliceous calc-hornfels unit is variably altered to tactite skarn (Jtc) along the margins of this intrusion.

Type 2 comprises the massive metadacite tuff (Jmdt) exposed on the western side of Empire Mountain, which has yielded ages of 185.0 ± 2.3 Ma, 188.8 ± 5 Ma, and 195.7 ± 1.4 Ma. This unit is lithologically quite uniform, and the 189 Ma and 196 Ma ages are derived from samples from the same area. The reason for the discrepancy in these ages is unknown. The 185 Ma age obtained from a sample near Timber Gap is chosen as most representative of this unit based on its central location in the unit and similarity to one of the other ages.

Type 3 comprises an unusual layered metadacite tuff and tuff breccia (Jslv) west of Spring Lake that has yielded dates of 183.3 ± 2.0 Ma and 170.9 ± 5 Ma. In map view, this unit is less elongate in shape than other units and is characterized by anomalously northeast-striking bedding with low dips, apparent open folds, and a distinctive series of white felsite dikes. An apparent boulder breccia with clasts >1 m in diameter was observed in a cliff face ~500 m west of Spring Lake. This unit has some characteristics of a caldera fill sequence, although the broad spread of ages suggests a more complex history.

Hornblende gabbros of two ages are present, including the youngest dated Jurassic rocks in the pendant. A coarse-grained hornblende gabbro unit (Jhb) exposed at Black Rock Pass on the eastern edge of the pendant has yielded a U-Pb zircon age of 182.5 ± 2.8 Ma. This is in the same age range as the metadacite tuff and associated rocks of Spring Lake (Jslv), but it is unclear if there is any direct relationship.

Similar hornblende gabbro (Jgb) exposed on the western side of Mineral King valley comprises the youngest rocks of the assemblage, with U-Pb zircon age of 161.8 ± 1.7 Ma. This unit is exposed as two parallel steeply dipping sills intruded into siliceous hornfels (Trsa). We interpret a smaller gabbro sill exposed in a steep dip slope on the southern flank of Empire Mountain to be correlative.

The two isolated slivers of dated Early Jurassic rocks include predominantly felsic volcaniclastic sedimentary rocks on Miners Ridge (Jvs) that yielded a suite of detrital zircon grains with a calculated maximum depositional age of ≤187 Ma (Attia et al., 2021). A well-bedded unit of calcareous quartzite, quartzofeldspathic sandstone, and variably reworked felsic tuffs (Jcsv) is present north of Eagle Lake and has yielded a U-Pb zircon age of 183.8 ± 1.7 Ma from a felsic tuff layer. These two units are similar lithologically to other pendant rocks, but neither has a clear stratigraphic or structural relationship to the rest of the pendant.

Age Gap 3

A significant hiatus of ~25 m.y. occurs between the Early Jurassic assemblage and voluminous metarhyolite tuffs (map units Kmrt1– Kmrt3) of the Early Cretaceous assemblage. Contacts between these assemblages are shown in orange on Figures 8 and 9.

Felsic volcanic rocks of the Early Cretaceous assemblage were emplaced during a short-lived eruptive phase at ca. 135 Ma and are in contact with a wide variety of older units, as indicated on Figures 8 and 9. A pronounced unconformity is exposed on the eastern side of Vandever Mountain, where metarhyolite tuff (Kmrt3) and conglomerate (Kcgl) overlie slate and phyllite of unit Psp. The Early Cretaceous volcanic assemblage and the underlying unconformable contact are folded into a tight synclinorium, with the bulk of Vandever Mountain forming the core of the fold (Figs. 3 and 4B).

A similar although less clear-cut relationship is exposed north of Franklin Creek on the eastern wall of Mineral King valley, where Triassic marble (Trm) wraps around the southeastern end of an apparent syncline in the Early Cretaceous metarhyolite tuff (Kmrt2), suggesting a folded angular unconformity between the Early Cretaceous and Triassic assemblages.

Downloaded from http://pubs.geoscienceworld.org/gsa/geosphere/article-pdf/20/4/1190/6584248/ges02748.1.pdf
by guest

On the northwestern edge of the pendant north of Cold Spring, the Early Cretaceous metarhyolite tuff (Kmrt1) is in contact with truncated Permian and Triassic units that also indicate angular discordance. On the eastern side of the pendant, two additional slivers of the Early Cretaceous volcanic assemblage (Kvcs) have been identified by U-Pb zircon dating, in pseudo-conformable contact with Jurassic calc- and calc-siliceous hornfels (Jch and Jcsh).

We interpret this age gap and associated structural discontinuity as primarily an angular unconformity, with the Early Cretaceous volcanic assemblage deposited on a basement of previously deformed and imbricated Permian to Jurassic volcanosedimentary rocks. Subsequent post–Early Cretaceous contractional deformation has produced tight folding in the Early Cretaceous volcanic assemblage and the underlying depositional surface and further tightened and deformed pre-existing structures in older units.

Early Cretaceous Assemblage

The Early Cretaceous assemblage is dominated by three massive metarhyolite tuff units (Kmrt1, Kmrt2, and Kmrt3; Figs. 6A and 6B) and a coeval sheared granodiorite intrusion (Kwc). These units, along with two deformed granitoids of similar age exposed south and west of the map area, were referred to as the "volcano-plutonic suite of Mineral King" by Sisson and Moore (2013). The assemblage as mapped herein also includes breccia and metaconglomerate units exposed on Vandever Mountain (Kvbr and Kcgl) and a number of felsic volcanic and volcaniclastic units variably reworked to quartzofeldspathic sandstone and calc-silicate hornfels (Kvcs). This assemblage is indicated in shades of pink on the geologic map (Fig. 3), and structural relations are illustrated in Figure 4.

The Early Cretaceous volcanic assemblage represents a major pulse of eruptive activity that was tightly concentrated around 135 Ma. Units of this age are interlayered with, or in contact with, all other assemblages in the pendant. The variety of adjacent (possibly originally underlying) older units, the local angular discordance and truncation of older units, and a lack of concentrated shearing along these contacts suggests that contacts with older units were originally depositional.

The seven units in this assemblage have yielded 11 U-Pb zircon dates ranging from 134 Ma to 137 Ma. The massive and continuous nature of the major rhyolite tuff units and the tight clustering of ages indicates a substantial intrusive and eruptive event at ca. 135 Ma. Magmatic rocks of this age are uncommon in other parts of the Sierra Nevada, where a magmatic lull is recognized between ca. 150 Ma and 120 Ma (Sisson and Moore, 2013; Klemetti et al., 2014; Cao et al., 2015; Paterson and Ducea, 2015; Attia et al., 2021).

The massive to moderately bedded metarhyolites (Kmrt1, Kmrt2, and Kmrt3) have a relict pyroclastic texture (Fig. 6A), are locally reworked to quartzfeldspathic sandstone, and include lenses of volcanic breccia. We have chosen to identify them as separate map units because exposures comprise three prominent physically separated zones in the central and western part of the pendant. These units are, however, indistinguishable on the basis of lithology, U-Pb zircon ages from the three units (136.5 ± 2.7 Ma, 135.5 ± 1.4 Ma and 134.2 ± 0.7 Ma, respectively) are identical within error, and trace element geochemistry shows no distinguishing features (Klemetti et al., 2014). Taken together, these units indicate a short-lived episode of massive felsic ignimbrite eruptions in a continental to shallow marine environment.

Sheared granodiorite of White Chief Mine (Kwc), a medium-grained biotite granodiorite with well-developed northwest-trending foliation and shearing, was emplaced into the western side of the pendant at 135.0 ± 1.0 Ma (Sisson and Moore, 2013), coeval with the voluminous rhyolite tuff eruptions. The granodiorite intruded into Triassic units to the east, with well-developed tactite skarns where granodiorite is in contact with marble of unit Trm (Sisson and Moore, 2013; Ryan-Davis et al., 2019).

A calc-silicate conglomerate with distinctive white felsite clasts (Kcgl) underlies the massive metarhyolite tuff unit (Kmrt3) on Vandever Mountain, whereas felsic volcanic breccia with angular clasts (Kvbr) overlies the metarhyolite tuff in the core of a major syncline (Figs. 3 and 4B).

Felsic volcanic and volcaniclastic sedimentary rocks interlayered with calc-silicate hornfels and volcanic breccia (Kvcs) are exposed in two lenses interleaved with Jurassic rocks on the eastern side of the pendant. One of these lenses, on the eastern side of Empire Mountain, has yielded a U-Pb age of 135.6 ± 1.3 Ma. The other, on the southern side of Mineral Peak, yielded a date of 135.4 ± 1.0 Ma. These dated units are lithologically similar to other felsic volcanic interlayers within the Jurassic calc-silicate hornfels units (Jcsh and Jch), suggesting that there are likely other as-yet-unidentified intercalations of Jurassic and mid-Cretaceous units within the pendant.

These dates, are, however, notably anomalous relative to those of adjacent strata interpreted as Jurassic. The date obtained east of Mineral Peak is especially unexpected considering that an age of 198 Ma was obtained from a similar felsic volcanic layer less than a kilometer to the north.

An alternative possibility for at least some parts of unit Kvcs is that some of the felsic volcanic interlayers, including those dated here, are sills intruded into older Jurassic rocks during the massive ignimbrite eruptions at 135 Ma. Based on field relations, however, especially the finely interstratified character of the felsic volcanic and adjacent reworked volcanosedimentary layers, we consider this possibility unlikely. Rather, we interpret these 135 Ma ages to provide an accurate age for the adjacent sedimentary layers.

Similar interlayered felsic volcanic and volcaniclastic sedimentary rocks are exposed on the western side of Vandever Mountain and yield an age of 134.2 ± 1.0 Ma. These are included in the Kvcs unit along with lithologically similar but undated units near Bullion Flat at the southern end of the mapped pendant.

Age Gap 4

Our dating indicates a hiatus of at least 16 m.y. subsequent to the major silicic eruptive phase at 135 Ma, before deposition of a reworked metarhyolite

Downloaded from http://pubs.geoscienceworld.org/gsa/geosphere/article-pdf/20/4/1190/6584248/ges02748.1.pdf
by guest

tuff and sandstone unit with a poorly constrained maximum depositional age of 118 Ma (Kmt) and intermediate and felsic volcanic rocks at 104.7 ± 1.0 Ma (Kma) and 100.5 ± 0.9 Ma (Kmrd), respectively. Contacts between these assemblages are shown in gray on Figures 8 and 9.

A discontinuity is present at all contacts between the middle Cretaceous assemblage and other units. For example, volcanic units west of Timber Gap (Kma) and north of Eagle Lake (Kmrd) have both yielded U-Pb zircon ages of ca. 100 Ma, but both are now steeply dipping and imbricated into sections of substantially older rocks, requiring a significant phase of post–100 Ma deformation. These contacts are noteworthy in that they involve felsic volcanic rocks interpreted as subaerial to shallow submarine ash-flow tuffs with U-Pb zircon ages of ≤118–101 Ma that are now in contact with plutonic rocks of only slightly younger ages.

Middle Cretaceous Assemblage

Rocks of middle Cretaceous age in the Mineral King pendant include three subaerially deposited metavolcanic units (Kmt, Kma, and Kmrd) and two intrusive bodies (quartz diorite of Empire Mountain and granodiorite of Spring Lake, Kem and Ksl, respectively). Rocks of this assemblage are indicated in shades of purple on the geologic map and cross sections (Figs. 3 and 4).

The oldest unit (Kmt; Fig. 6D) consists of mixed and reworked volcaniclastic rocks including felsic tuffs, breccias, and quartzofeldspathic sandstone exposed on the northwestern edge of the pendant. Kmt has yielded a poorly constrained detrital zircon maximum depositional age of ≤118 Ma. This unit is intruded by the quartz diorite of Empire Mountain (Kem), indicating that its age must be older than 106 Ma.

The two younger mid-Cretaceous felsic volcanic units (Kma and Kmrd) are isolated and structurally interleaved with older strata. We interpret these discordant contacts to indicate fault imbrication into older units during flattening and vertical extension, in association with emplacement of Cretaceous plutons. Kma comprises metamorphosed andesitic lava flows, breccias, and interleaved felsic volcanic rocks west of Timber Gap. Kma rocks are lithologically similar to dated Triassic andesitic volcanic rocks to the southeast (e.g., Trma) and are bounded on both sides by dark gray siliceous hornfels of presumed Triassic age (Trsa), allowing the interpretation that Kma is infolded into the core of a (probably faulted) isoclinal syncline (Fig. 4A). A fold hinge has not been observed, however, so an isoclinal fold, if present, is likely modified by faulting and distributed ductile flattening deformation. Repeated sampling of interleaved felsic tuff on the western edge of this unit has yielded U-Pb zircon ages of 110.6 ± 3 Ma, 104.7 ± 1.0 Ma, and 99.0 ± 2.0 Ma, confirming its mid-Cretaceous age.

Metarhyolite tuff interlayered with volcanogenic sandstone and mixed dacitic tuffs (Kmrd) exposed north of Eagle Lake near the western edge of the pendant has yielded a U-Pb zircon age of 100.5 ± 0.9 Ma. This is an anomalously northeast-striking block between Jurassic units dated at ≤187 Ma (Jvs) and 184 Ma (Jcsv). There is no evidence of a fold hinge and distinctive lithologies within the block are not repeated, indicating that this block is likely fault bounded on one or both sides.

Quartz diorite of Empire Mountain (Kem) appears to have intruded the pendant as a now-vertical sill that split apart pre-existing steeply dipping metasedimentary units (Fig. 3). The Kem unit yields U-Pb zircon ages of 106.2 ± 1.1 Ma and 108.5 ± 1 Ma and was emplaced at a depth of ~3.3 km (D'Errico et al., 2012). We interpret this intrusive unit as structurally part of the pendant rather than the bounding Late Cretaceous plutons because (1) it is northwest elongate with steeply dipping contacts; (2) its southern half is bounded on both sides by pendant strata into which it has forcefully intruded as a layer-parallel sill; and (3) it is significantly older than the bounding Late Cretaceous plutons, with an age that overlaps with and/or is older than that of the youngest metavolcanic strata exposed in the pendant to the west.

The granodiorite of Spring Lake (Ksl), exposed to the east of Kem, has yielded a U-Pb age of 104.2 ± 1.4 Ma. It has been suggested to be a lighter-colored facies of the quartz diorite of Empire Mountain (Sisson and Moore, 2013), but this is unlikely given the 4 m.y. difference in age.

It is noteworthy that these two shallow- to mid-crustal plutons (Kem and Ksl) are very close in age to andesitic and interleaved felsic volcanic rocks 2–3 km to the west near Timber Gap that have pyroclastic textures indicative of surficial deposition at ca. 105 Ma. Similarly, the metarhyolite tuff unit exposed on the eastern side of Miners Ridge (Kmrd) has an age of 100.5 ± 0.9 Ma, yet the granodiorite of Castle Creek (Kcc), which bounds the pendant 0.4 km to the west, is dated at 98 ± 1 Ma (Sisson and Moore, 2013) and was emplaced at a depth of ~11 km (Klemetti et al., 2014). Thus, plutons emplaced at mid-crustal levels are yielding ages only 1–2 m.y. younger than, and within error of, those of silicic volcanic rocks deposited at the Earth's surface that are presently vertically dipping and interleaved within the pendant stratigraphy. Similar short time intervals between surficial volcanic rocks and adjacent mid-crustal plutons have been documented in other Sierran pendants (e.g., Saleeby, 1990; Cao et al., 2016; Krueger and Yoshinobu, 2018; Ardill et al., 2020).

The pendant is bounded by large Middle Cretaceous plutons, the granodiorite of Castle Creek (Kcc) and the granite of Coyote Pass (Kcp) and associated units (Kf, Kmcp, Kcciz and Kap, Sisson and Moore, 2013).

STRUCTURE OF THE MINERAL KING PENDANT

The Mineral King pendant is characterized by northwest-striking, steeply dipping lithologic units with variably developed but generally prominent layer-parallel cleavage and flattening foliation and steeply plunging stretching lineation. The well-developed, steeply dipping planar fabric gives the pendant a typically striped appearance with jagged, cliffy outcrops. Exposures are abundant and clearly visible but not always accessible.

The overall structural pattern is complex (Fig. 10). Lithologic units are typically discontinuous at outcrop to map (meter to kilometer) scales and change along strike due to a combination of facies changes, structural attenuation, and

Downloaded from http://pubs.geoscienceworld.org/gsa/geosphere/article-pdf/20/4/1190/6584248/ges02748.1.pdf
by guest

Figure 10. Crystal Creek drainage and east face of East Fork Kaweah River valley showing map units and relationships. Image shows ~2 km horizontally and 1 km vertically.

faulting. Tight to isoclinal folds are locally evident at meter to kilometer scales (Fig. 11), and U-Pb dating indicates extensive cryptic faulting and structural imbrication down to the 100 m scale (Figs. 9A and 12). Dismembered folds, discontinuous transposed bedding, and boudinage of competent layers are common. Folding and bedding transposition are likely ubiquitous although not uniformly visible in outcrop.

We interpret most structural relationships in the pendant to result from fault imbrication, isoclinal folding, and bedding transposition in a strain environment characterized by strong northeast-southwest shortening and vertical elongation. This structural architecture formed predominantly after 100 Ma given that the youngest dated unit in the pendant, mixed felsic metavolcanic rocks (Kmrd, 100.5 ± 0.9 Ma) west of Eagle Creek, is tilted to vertical dips and contains steeply dipping, layer-parallel foliation. Older units were likely deformed earlier, however, and the presently observed structural fabric across the pendant may represent the result of repeated parallel deformation.

We emphasize that detailed dating is critical for interpreting structure in the pendant. Lithologies are repetitive and non-diagnostic. The rocks are complexly deformed and structurally interleaved, and adjacent units display significantly different U-Pb ages that are difficult to predict from field context. Accurate structural interpretation requires detailed dating of individual layers at a scale comparable to the desired scale of interpretation.

Structural Fabric

Foliation

Foliation in the Mineral King pendant is variably developed but nearly ubiquitous and is defined by a combination of compositional layering, transposed bedding, cleavage, and flattening of clasts and inclusions. Foliation is

Downloaded from http://pubs.geoscienceworld.org/gsa/geosphere/article-pdf/20/4/1190/6584248/ges02748.1.pdf
by guest

Figure 11. View of Farewell Gap and surrounding peaks, looking southeast. Tight folding is visible in Cretaceous metavolcanic units on Vandever Mountain and in rusty-weathering Triassic metasedimentary units east of Farewell Gap. Horizontal field of view at skyline is ~3.5 km. Dashed white lines indicate 100-m scale folds visible in Triassic metasedimentary units.

generally northwest striking and steeply dipping with an average orientation of N23°W dipping 86°SW (Fig. 13).

Despite regional metamorphism to greenschist facies, original compositional layering (bedding) is generally well preserved at the outcrop scale, with original volcanic and volcaniclastic textures, fine sedimentary laminations and cross-lamination, and graded beds locally preserved in outcrop. Close examination, however, reveals that individual layers are commonly discontinuous at the meter scale, with evidence of flattening and down-dip elongation in the form of boudinage in stiffer layers, local decimeter-scale tight to isoclinal folding, and well-developed flattening fabrics (Fig. 14). Top-direction indicators, where visible, are in some cases conflicting at the meter scale.

Cleavage development is primarily controlled by lithology, with finer-grained and more micaceous units (e.g., Psp and Trsa) showing strongly developed fine slaty to schistose cleavage that obscures all other planar fabric (e.g., Fig. 5B), whereas coarser-grained, more massive units (e.g., Pvs and Trma) show more variably developed spaced cleavage. Flattening fabrics are especially well developed in volcaniclastic units, defined by preferred orientation of planar minerals and flattening and down-dip elongation of pumice and lithic clasts (Fig. 15).

Aplite dikes and rare mafic dikes commonly show chocolate-tablet boudinage with greater elongation in the down-dip direction. Aplite dikes intruding metarhyolite tuff (Kmrt1) west of Timber Gap are dismembered into individual elongate boudins in a broad zone of shearing, flattening, and down-dip elongation (Figs. 16A and 16B). These boudins have yielded a U-Pb age of 114.8 ± 3.1 Ma, which is younger than the 136.5 ± 2.7 Ma age of the enclosing rhyolite tuff but older than the 97.8 ± 0.7 Ma age of the adjacent granodiorite of Castle Creek (Sisson and Moore, 2013) that bounds the pendant to the west.

Downloaded from http://pubs.geoscienceworld.org/gsa/geosphere/article-pdf/20/4/1190/6584248/ges02748.1.pdf
by guest

Figure 12. View of ridge west of Timber Gap. Complex interlayering of units with diverse ages indicates fault imbrication, although indications of significant shear zones are only locally present. See also Figures 4A and 9A for cross-section interpretations. Horizontal field of view is ~700 m at ridge crest.

Lineation

Steeply plunging stretching lineation is prominently developed in much of the pendant and is defined by flattened and elongate pumice fragments in volcanic rocks, elongate clasts in volcanic breccias, and smearing of micaceous minerals on cleavage planes (Fig. 17). Lineation is primarily steeply northwest plunging, with an average orientation of N65°W plunging 83° (Fig. 13).

Strain Indicators

Ductile flattening and down-dip elongation are observed in all units of the Mineral King pendant, with intensity of deformation and fabric development dependent primarily on lithology. Discrete mylonitic shear zones with significant localized strain are rare in the pendant and difficult to distinguish from the general pattern of deformation.

Ductile flow fabrics are locally well developed around rigid porphyroclasts and show symmetric "phi-type" pressure shadows (Fig. 16). We observed no evidence for a consistent asymmetry in either horizontal or lineation-parallel surfaces.

Fabric in the Granodiorite of White Chief Mine

The granodiorite of White Chief Mine (Kwc) was emplaced along what is now the southwestern edge of the pendant at 135 ± 1 Ma (Sisson and Moore,

Downloaded from http://pubs.geoscienceworld.org/gsa/geosphere/article-pdf/20/4/1190/6584248/ges02748.1.pdf
by guest

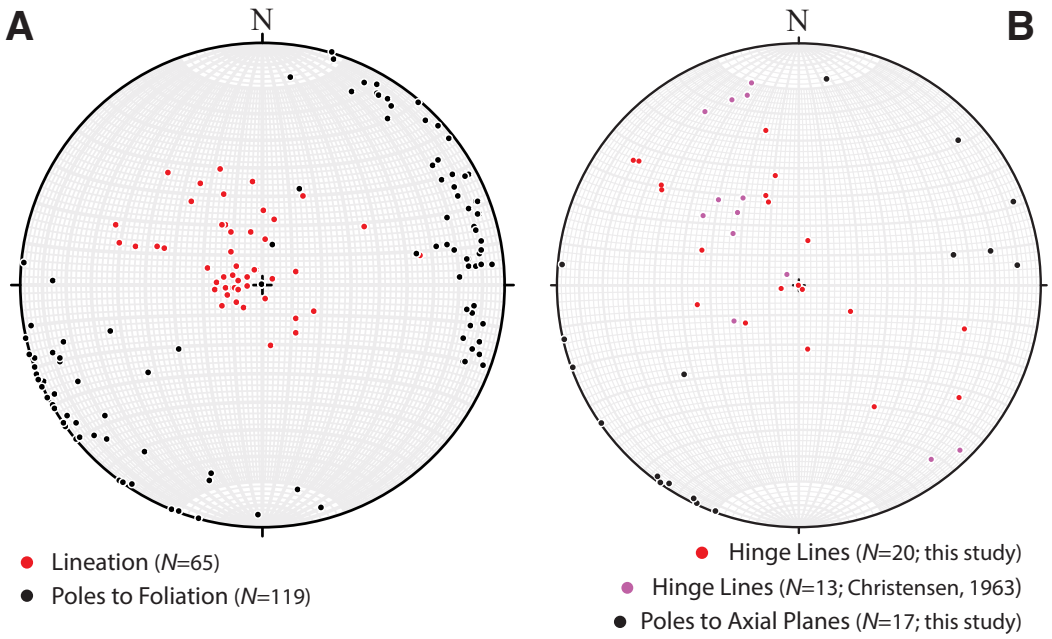

Figure 13. Equal-area stereonets showing structural orientations in the Mineral King pendant, California, USA. (A) Orientations of foliation and lineation. Average orientation of foliation is 337° dipping 86° to the southwest. Average orientation of lineation is 295° plunging 83°. (B) Orientations of fold hinge lines and axial planes. Stereonets were constructed using Stereonet v. 11.5.4 (Allmendinger et al., 2012; Cardozo and Allmendinger, 2013).

2013) and thereafter behaved structurally as part of the pendant. The granodiorite contains a well-developed, northwest-striking foliation (Fig. 18) with down-dip lineation that is parallel to that in the rest of the pendant.

Localized zones of ductile deformation trend northwest and are parallel to foliation in the pluton (Worm and Greene, 2016). These zones range from distributed millimeter-thick zones of protomylonite to decimeter-thick, gray-green, very fine-grained bands of ultramylonite (Fig. 18B) spaced tens of meters apart that both crosscut and are crosscut by aplite dikes.

In thin section, undeformed grains are elongate in a northwest direction, with evidence of crystal-plastic deformation along grain boundaries. Elongate stringers of quartz in ductilely deformed zones show distinct sub-grains. Strain indicators are generally symmetric, and we observed no evidence for a preferred direction indicative of simple shear. We interpret these observations to be consistent with post-emplacement ductile deformation of the White Chief pluton, likely concurrent with the major phase of mid-Cretaceous deformation in the Mineral King pendant.

Folding

The significance of large-scale folding and bedding transposition in the Mineral King pendant was recognized by Christensen (1963, p. 159), who described "major isoclinal folds with subhorizontal axes and nearly vertical limbs". In contrast, Busby-Spera (1983) and Busby-Spera and Saleeby (1987) recognized folding locally in outcrop but considered it to be intraformational and insignificant within an overall intact homoclinal stratigraphic package. Sisson and Moore (2013), following on the unpublished field mapping of J. Dillon and students in 1969 (T. Sisson, 2011, personal commun.), mapped a major northwest-trending syncline on Vandever Mountain as well as significant kilometer-scale folding in the Tulare Peak and Monarch Lakes areas. Our work further supports the interpretation that tight to isoclinal folding and transposed bedding are primary structural elements at all scales in the Mineral King pendant. Following is discussion of significant areas of folding in the Mineral King pendant.

Kilometer-Scale Folding

Folding on Vandever Mountain. The characteristic kilometer-scale folding at Mineral King is well exposed on Vandever Mountain where a 2-km-long northwest-trending synclinorium in 134 Ma metarhyolite (Kmrt3) underlies the ridge crest (Figs. 3 and 4B). The overall structure is that of a tight, upright, shallowly south-plunging syncline cored by rhyolite tuff (Kmrt3) and volcanic breccia (Kvbr), with the conglomerate unit Kcgl exposed on the ridge north of

Downloaded from http://pubs.geoscienceworld.org/gsa/geosphere/article-pdf/20/4/1190/6584248/ges02748.1.pdf
by guest

Figure 14. Folded and transposed bedding in calc-silicate hornfels. Unit Jcsh in Monarch Lakes basin (36.4510°N, 118.5650°W). Jackknife is 9 cm in length.

Figure 15. Flattening fabric in heterolithologic breccia interbedded with Early Cretaceous metarhyolite tuff. Image is a vertical face, perpendicular to foliation and parallel to lineation. Unit Kmrt2 southeast of Timber Gap (36.4658°N, 118.5923°W). Coin is 2 cm in diameter.

the summit delineating the nose of the structure. Subsidiary tight folds parallel to the main structure are visible in cliffs northwest of the summit (Fig. 19). The syncline is cut out to the south by younger mid-Cretaceous plutons.

On the western wall of Farewell Canyon, the Cretaceous volcanic rocks (Kmrt3 and Kcgl) unconformably overlie older Permian clastic units (Fig. 19A), and this unconformity surface was subsequently tightly folded along with the Early Cretaceous volcanic strata. The nose of the syncline and the folded unconformity surface are exposed on the ridge northwest of Vandever Mountain (Fig. 3), although complicated in detail by localized shearing.

Southeast of Vandever Mountain, undated wedges correlated with the Cretaceous volcanic assemblage are exposed within Permian slate and phyllite (Psp) both west and east of Bullion Flat (Fig. 3). This outcrop pattern is consistent with a series of kilometer-scale tight folds of the mid-Cretaceous unconformity surface, resulting in tight infolds of Cretaceous felsic volcanic rocks within the Permian clastic unit.

Folding northwest of Bullfrog Lakes. A 2.5-km-long, northwest-trending, tight to isoclinal, fault-bounded syncline and associated smaller folds are exposed northwest of Bullfrog Lakes on the west face of Tulare Peak (Fig. 3). The primary syncline is cored by siliceous hornfels (Trsa), which has yielded Triassic fossils (as well as Jurassic fossils interpreted to be out of place; Busby-Spera and Saleeby, 1987). The limbs of the syncline, as well as a series of parallel subsidiary folds, are exposed in arkosic metasandstone (Trss) that has yielded a Middle Triassic detrital zircon maximum depositional age of ≤239 Ma (Attia et al., 2021).

This fold sequence is upright, with axial-plane orientations parallel to steeply dipping, northwest-striking cleavage. Hinge-line orientations are

Downloaded from http://pubs.geoscienceworld.org/gsa/geosphere/article-pdf/20/4/1190/6584248/ges02748.1.pdf
by guest

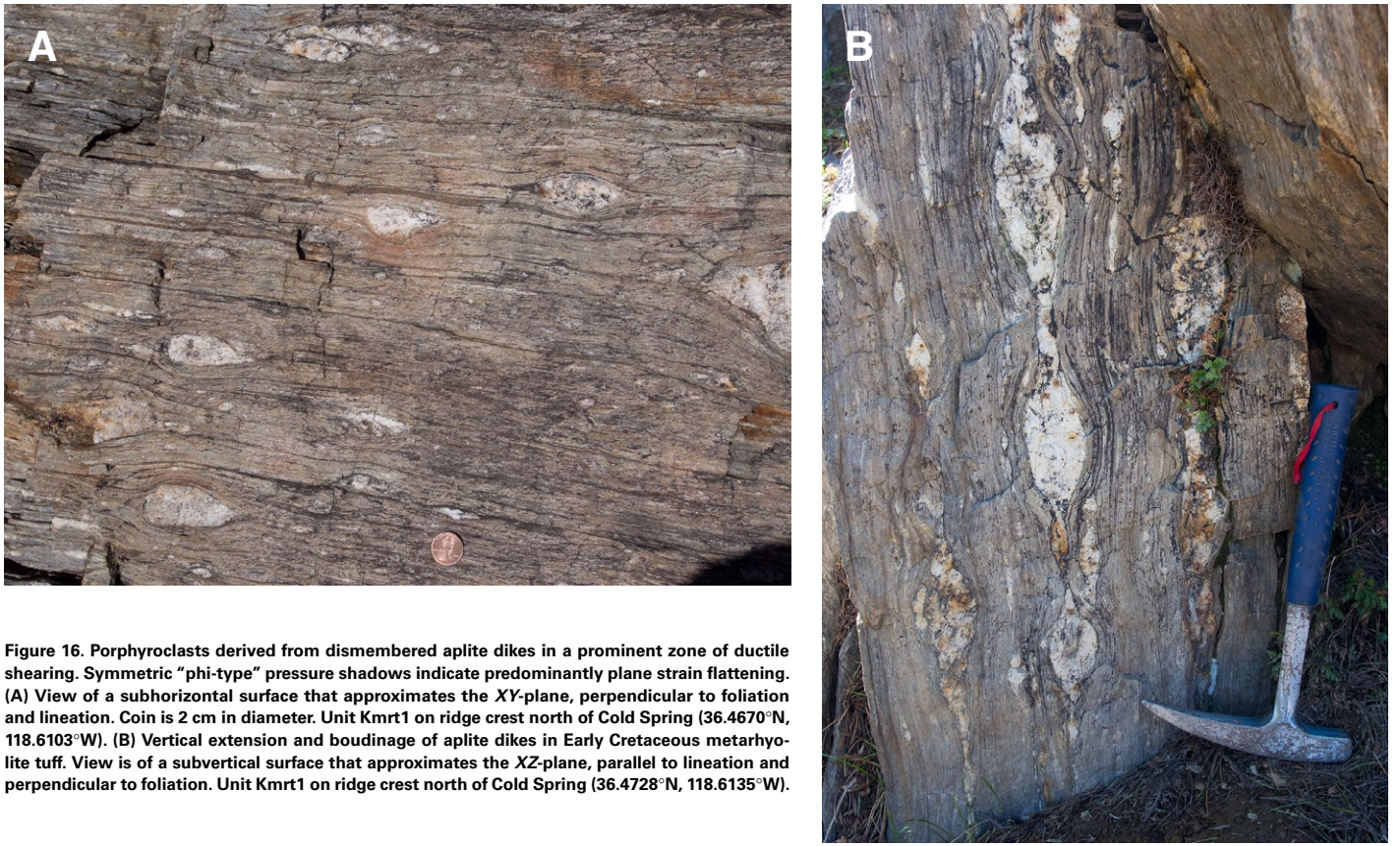

Figure 16. Porphyroclasts derived from dismembered aplite dikes in a prominent zone of ductile shearing. Symmetric "phi-type" pressure shadows indicate predominantly plane strain flattening. (A) View of a subhorizontal surface that approximates the *XY*-plane, perpendicular to foliation and lineation. Coin is 2 cm in diameter. Unit Kmrt1 on ridge crest north of Cold Spring (36.4670°N, 118.6103°W). (B) Vertical extension and boudinage of aplite dikes in Early Cretaceous metarhyolite tuff. View is of a subvertical surface that approximates the *XZ*-plane, parallel to lineation and perpendicular to foliation. Unit Kmrt1 on ridge crest north of Cold Spring (36.4728°N, 118.6135°W).

variable but generally shallow to moderately northwest plunging, for example, northwest of Tulare Peak where topography and exposure imply a minimum plunge of 30°NW for the adjacent anticline.

Folding in this area must have been post–Late Triassic in age based on the age of the folded rocks. South of Bullfrog Lakes, folds are cut by the Cretaceous granite of Coyote Pass (Kcp), indicating that deformation occurred prior to 99 Ma.

The folds north of Bullfrog Lakes are similar in scale, orientation, and style to those on Vandever Mountain, including a primary syncline with height and width (half amplitude and half wavelength, respectively) in excess of 0.5 km and exposed strike lengths of >2 km. Both areas typically show development of parallel subsidiary folds in adjacent units, and indeed these may all be part of a continuous fold train based on interpreted folds in the intervening Permian clastic units (Psp and Pvs) (Figs. 3 and 4B). In this case, the entire fold train in this southern part of the pendant would be mid-Cretaceous in age, with deformation constrained to post–135 Ma and pre–99 Ma.

At least one previous generation of deformation is likely, however, given that the Early Cretaceous volcanic assemblage unconformably overlies a variety of older units with ages ranging from late Permian to Early Jurassic, implying that previous deformation and erosion had produced a depositional surface with a variety of exposed units and ages.

Folding northwest of Franklin Lakes. A tight to isoclinal synclinal fold cored by metarhyolite tuff (Kmrt2) is exposed in the cliff face north of Franklin Creek (Fig. 10). Folded original layering in the metarhyolite tuff is not apparent in the poorly layered (and largely inaccessible) exposures, but the presence of older Triassic marble (Trm) wrapping around the southern end of the Kmrt2 unit supports the presence of a fold (Sisson and Moore, 2013). This syncline apparently dies out to the northwest before reaching the Monarch Creek drainage.

Downloaded from http://pubs.geoscienceworld.org/gsa/geosphere/article-pdf/20/4/1190/6584248/ges02748.1.pdf
by guest

Figure 17. Steeply plunging stretching lineation, here defined primarily by smearing of micaceous mineral grains. View is of subvertical surface approximating the *XY*-plane, parallel to foliation and lineation. Unit Trma on south side of Monarch Creek (36.4559°N 118.5846°W). Jackknife is 9 cm in length.

Folding west of Timber Gap. On the prominent ridge west of Timber Gap (Fig. 12), a 1-km-long lens of siliceous argillite of Triassic(?) age (Trsa) is surrounded by slate and phyllite correlated with unit Psp to the southeast (Fig. 3). If these lithologic correlations are correct, this relationship suggests an isoclinal syncline of Triassic strata infolded into Permian strata, similar to the structural relationship in Triassic strata on Tulare Peak to the southeast.

Farther to the west along this ridge, Trsc and Trm appear to be infolded into Pvt, and these units are truncated at the contact with metarhyolite tuff (Kmrt1). We interpret this contact as an angular unconformity analogous to that at the base of Early Cretaceous metarhyolite tuff (Kmrt3) on Vandever Mountain.

100-Meter-Scale Folding

Tight folds with half wavelengths in the range of 50–200 m are locally developed in well-bedded units throughout the Mineral King pendant. Especially well-developed folding is apparent in well-bedded Triassic metasandstone (Trss) and siliceous hornfels (Trsa) northwest of Bullfrog Lakes (Fig. 3), in metaconglomerates (Kcgl) on the ridge northwest of Vandever Mountain (Fig. 19), and in bedded marble and calc-silicate hornfels (Trm and Trsc) west and northwest of the lower Franklin Lake (Figs. 20A and 20B).

Figure 18. (A) Fabric in granodiorite of White Chief Mine (Kwc), interpreted to result from syn-emplacement deformation. View is of *YZ*-plane, perpendicular to foliation and lineation. Horizontal field of view is 12 cm (36.4258 °N, 118.6002 °W). (B) Ultramylonite band in sheared granodiorite of White Chief Mine (Kwc), showing isolated porphyroclasts of granodiorite. View is of *YZ*-plane, perpendicular to foliation and lineation. Jackknife is 9 cm in length (36.4246°N, 118.6000°W).

Downloaded from http://pubs.geoscienceworld.org/gsa/geosphere/article-pdf/20/4/1190/6584248/ges02748.1.pdf
by guest

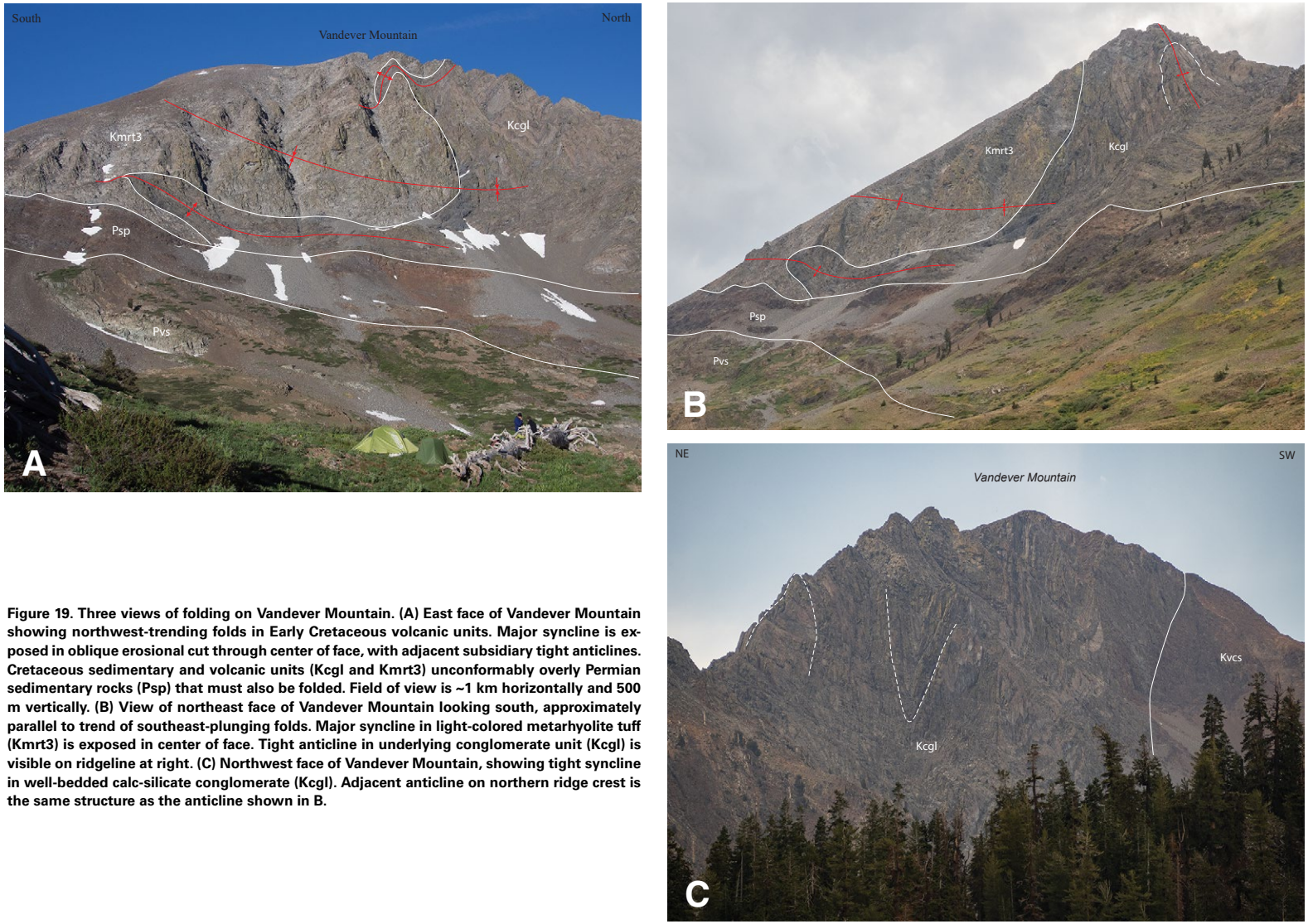

Figure 19. Three views of folding on Vandever Mountain. (A) East face of Vandever Mountain showing northwest-trending folds in Early Cretaceous volcanic units. Major syncline is exposed in oblique erosional cut through center of face, with adjacent subsidiary tight anticlines. Cretaceous sedimentary and volcanic units (Kcgl and Kmrt3) unconformably overly Permian sedimentary rocks (Psp) that must also be folded. Field of view is ~1 km horizontally and 500 m vertically. (B) View of northeast face of Vandever Mountain looking south, approximately parallel to trend of southeast-plunging folds. Major syncline in light-colored metarhyolite tuff (Kmrt3) is exposed in center of face. Tight anticline in underlying conglomerate unit (Kcgl) is visible on ridgeline at right. (C) Northwest face of Vandever Mountain, showing tight syncline in well-bedded calc-silicate conglomerate (Kcgl). Adjacent anticline on northern ridge crest is the same structure as the anticline shown in B.

Fold axial planes are generally northwest striking and steeply southwest dipping, parallel to foliation. Hinge-line orientations are variable, generally northwest-southeast trending with plunges varying from shallow to steep (Fig. 13B).

A complexly folded zone in orange-weathering interbedded calc-silicate hornfels and marble (Trsc) is well exposed but inaccessible on the east face of Mineral King valley east of Soda Springs (Fig. 10). Folds are delineated by gray-weathering marble layers within the orange siliceous hornfels. The irregular pattern of highly elongate folds appears to result from tight folds with hinge lines subparallel to the exposure face making very oblique cross sections of fold traces.

Downloaded from http://pubs.geoscienceworld.org/gsa/geosphere/article-pdf/20/4/1190/6584248/ges02748.1.pdf
by guest

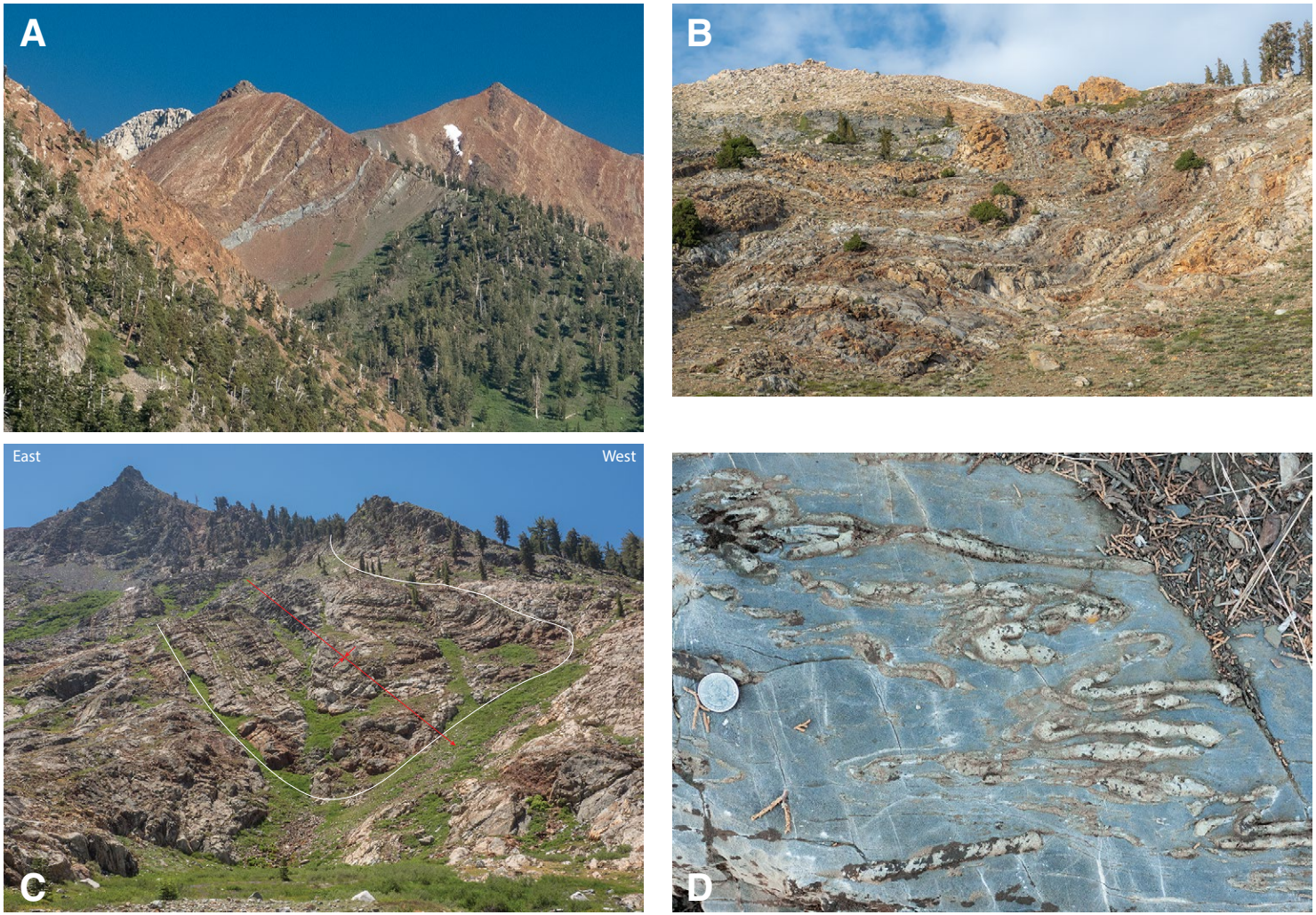

Figure 20. Examples of 100-m-scale to outcrop-scale folding in Mineral King pendant, California, USA. (A) Tight to isoclinal folding delineated by gray carbonate layer, exposed in unit Trsc on face south of Franklin Creek. Width of fold is ~50 m. (B) Complex folding in interbedded marble and calc-silicate hornfels of unit Trm, northwest of lower Franklin Lake (36.4266°N, 118.5673°W). Horizontal field of view is ~150 m. (C) South-plunging, faulted syncline in layered siliceous calc-hornfels of unit Jch, exposed on southern wall of Monarch Creek. Width of fold is ~100 m. (D) Rootless isoclinal folding in gray marble with calc-silicate interbeds. Exposed on Monarch Lakes trail in unit Trsa (36.4557°N, 118.5947°W). Diameter of coin is 2.5 cm.

Downloaded from http://pubs.geoscienceworld.org/gsa/geosphere/article-pdf/20/4/1190/6584248/ges02748.1.pdf
by guest

North of Mineral Peak in units Jcsh and Jch, bedding is less steeply dipping than elsewhere in the pendant, and folding is more open and plunges shallowly to moderately northwest. This area on the eastern side of the pendant is separated from more steeply dipping areas of the pendant to the west by an east-dipping shear zone. West of this shear zone, tight, faulted folds are evident in well-bedded calc-silicate hornfels (Jch) on the southern side of Monarch Creek (Fig. 20C).

Outcrop-Scale Folding

Tight folding, boudinage, and discontinuous bedding on a decimeter scale are characteristic of many thin-bedded units in the Mineral King pendant (e.g., Fig. 14). Marble has behaved ductilely throughout the pendant (Fig. 20D), and well-developed folding is especially evident in units with interbedded marble. Folds are characteristically upright, with northwest-striking, steeply dipping axial planes and hinge lines that plunge variably to the northwest and southeast. These smaller folds may have responded more readily than the larger folds to late-stage ductile strain, with local reorientation of pre-existing folds to steeper plunges closer to the stretching direction during mid-Cretaceous flattening and vertical elongation.

Faults

Major faults and shear zones in the Mineral King pendant are expressed primarily as age discontinuities documented by U-Pb zircon dating and commonly have little to no outcrop expression. Strata are tilted to near-vertical dips, and steeply dipping, layer-parallel ductile flattening foliation and steeply plunging stretching lineation are broadly but irregularly developed throughout the pendant. Fabric development depends primarily on lithology and is most intensely developed in micaceous units and at lithologic boundaries with rheological contrasts.

Structural overprint has reduced the fabric contrast between more- and less-deformed zones and obscured mylonitic fabrics that might identify major shear zones. We have observed few shear-sense indicators in pendant rocks and no unambiguous textural evidence for faults or shear zones with significant displacement. The presence of such faults or shear zones does, however, seem to be required by the age discontinuities documented by our U-Pb dating.

In the following section, we discuss faults previously mapped in the Mineral King pendant based on topographic and outcrop expression along with our field observations and interpretations. We use the term "fault" broadly and in its historical sense to indicate any tabular zone along which there is (or has been proposed to be) significant shear displacement, either brittle or ductile. However, almost all proposed faults in the Mineral King pendant have significant width and at least some evidence for ductile deformation and could also be described as shear zones.

Previously Defined Faults

A number of major brittle to brittle-ductile faults have been previously mapped in the Mineral King pendant (unpublished mapping of J. Dillon and students, T. Sisson, 2011, personal commun.; Busby-Spera, 1983; Busby-Spera and Saleeby, 1987; Sisson and Moore, 2013).

Empire fault. The Empire fault as defined by Busby-Spera and Saleeby (1987) is a zone of brittle shear in the northern part of the pendant that separates Early Cretaceous metarhyolite tuff (Kmrt2) with a U-Pb zircon age of 136 Ma from Jurassic metadacite tuff (Jmdt) with a U-Pb zircon age of 185 Ma. South of Monarch Creek, they interpreted this fault as forming the boundary between Triassic meta-andesite (Trma) and Jurassic calc-silicate hornfels (Jch and Jcsh), truncated to the southeast by the mid-Cretaceous granodiorite of Coyote Pass (Kcp). Kistler (1990) suggested that this fault represented a segment of the Panthalassan–North American lithosphere boundary.

Although we interpret this zone as a significant discontinuity, we find little evidence for a continuous Empire fault zone. North of Timber Gap, the contact between Cretaceous metarhyolite tuff and Jurassic metadacite tuff is locally strongly foliated, but evidence for a continuous shear zone is lacking (Sisson and Moore, 2013; our mapping). We interpret this contact as an angular unconformity, with Cretaceous metarhyolite tuff (Kmrt2) originally deposited on deformed Triassic and Jurassic strata.

South of Monarch Creek, localized brittle deformation is present at the contact between massive meta-andesite (Trma) and layered calc-siliceous metasedimentary strata (Jch). Shearing would be expected at this strong rheological contrast, but we have observed no evidence of significant displacement.

Farther south along this contact, a thick (>10 m) zone of highly foliated rock is developed south of Crystal Creek and is truncated by the mid-Cretaceous granodiorite of Coyote Pass. We concur with previous workers (Busby-Spera and Saleeby, 1987; Sisson and Moore, 2013) that this represents a significant shear zone. In our interpretation, however, the shear zone swings northward into the upper Monarch Creek drainage, forming the boundary between Jurassic calc-hornfels and calc-siliceous hornfels units (Jch and Jcsh). This trace is in part similar to that of the Mineral fault of Busby-Spera and Saleeby (1987).

Mineral Peak fault. A north-striking, moderately to steeply east-dipping zone of intense cleavage development is exposed in the cirque northwest of Mineral Peak where it separates unit Jcsh from Jch. This shear zone appears to be a significant boundary, separating a region of moderately east-dipping strata with more open folding on the eastern edge of the pendant (Jcsh and Jslv) from the more steeply dipping and tightly folded rocks in the central and western areas of the pendant. The Mineral Peak fault as mapped here (Fig. 3) is similar to that mapped by Busby-Spera (1983) and named the Mineral fault but differs in specific location.

On the ridge west of Mineral Peak, a hanging-wall syncline is visible east of the shear zone. Where the shear zone intersects the Monarch Lakes trail,

Downloaded from http://pubs.geoscienceworld.org/gsa/geosphere/article-pdf/20/4/1190/6584248/ges02748.1.pdf
by guest

mylonitic foliation is moderately east dipping, and sparse shear indicators support east-down normal displacement. The zone is hydrothermally altered, with tactite and skarn mineralization prominent in a 100-m-wide zone coincident with the shear zone (Christensen, 1963).

The quartz diorite of Empire Mountain (Kem) and a subsequently intruded north-south-trending dike of Kmcp both appear to have intruded into this zone of weakness, wedging apart the Jch unit. Bedding and foliation in unit Jch in the Monarch Creek drainage west of the Kem intrusion show anomalously west-northwest orientations, whereas bedding and fold hinge lines east of the intrusion are bent to the north. Both orientations are consistent with deflection around the southern tip of the Empire Mountain intrusion.

Farewell fault. Previous geologic maps of Mineral King pendant and the southern Sierra Nevada region show a north-northwest-striking fault zone called the Farewell fault bisecting the pendant. The fault trace extends from south of Farewell Gap north through Farewell Canyon and Mineral King valley and across the ridge west of Timber Gap (e.g., Busby-Spera, 1983; Saleeby and Busby, 1993; Nadin and Saleeby, 2008; Sisson and Moore, 2013). The fault zone, as mapped in these sources, coincides with a steeply dipping zone of highly cleaved, fine- to very fine-grained slates and phyllites exposed at Farewell Gap and in the deeply eroded gully of Farewell Canyon. The proposed fault is unexposed in the floor of Mineral King valley but could be connected with any of a number of highly cleaved slates and phyllites on the ridge west of Timber Gap.

Evidence of shearing is locally present in slates at Farewell Gap and in a zone of schistose metarhyolite west of the gap, but in other locations along the mapped fault zone, rocks are not strongly sheared (Sisson and Moore, 2013; our mapping). Steeply plunging asymmetric folds of slaty cleavage within the fault zone have been interpreted to indicate dextral displacement (Busby-Spera, 1983; Saleeby and Busby, 1993).

The spectacular northwest-trending linear topographic valleys of the Little Kern River, Farewell Gap and Farewell Canyon, the East Fork Kaweah River, and Timber Gap Creek that coincide with the trend of this fault zone (Figs. 2 and 3) have contributed to the interpretation that the Farewell fault could be an exposed segment of a major dextral shear zone in the southern Sierra Nevada (e.g., Schweickert and Lahren, 1991; Kistler, 1993; Nadin and Saleeby, 2008). However, there is no direct evidence for differential displacement along this inferred fault zone. The trace of the fault is located largely within slate and phyllite of a single map unit (Psp) in Farewell Canyon, and elsewhere mapped units on either side of the fault zone are similar.

The fault trace to the north and south of Farewell Gap is locally marked by springs and tufa deposits, but south of Farewell Gap, the projected trace of the fault is cut by a Cretaceous metarhyolite tuff and an aplite pluton that do not show significant offset (Sisson and Moore, 2013). Exposures of the Early Cretaceous volcanic assemblage are present on both sides of the Farewell fault zone. Rocks of this age (ca. 135 Ma) are uncommon in the Sierra Nevada, and Sisson and Moore (2013) suggested that the cluster of such units in and near Mineral King is the result of an original magmatic center, and thus the individual units are unlikely to be far traveled.

The present expression of the Farewell fault appears to be primarily a late brittle fracture system formed parallel to steeply dipping regional foliation. The topographic expression of this fault has been accentuated by strike-parallel differential stream erosion into steeply dipping and highly cleaved strata, as, for example, in the slates and phyllites (Psp) in Farewell Canyon and in vertically dipping marble interbedded with siliceous hornfels (Trsa) north of Timber Gap.

Other Mapped Faults

A pair of northwest-striking, steeply dipping faults northwest of Bullfrog Lakes are localized at the boundary between Triassic metasandstone (Trss) and siliceous hornfels (Trsa) and are likely associated with the tight folding in this area. We also map a northeast-striking late brittle fault in the Monarch Creek drainage with ~50 m of left-lateral offset of a Late Cretaceous diorite sill (Kmcp).

The generally northeast-striking contact between the Early Cretaceous volcanic assemblage (Kvcs and Kcgl) and older Triassic volcanic and calc-silicate strata (Trvc and Trsc) on the ridge crest north of Vandever Mountain was mapped by J. Dillon and students (T. Sisson, 2011, personal commun.) as the intersection of a south-plunging synformal fold hinge with topography. This contact was later interpreted by Busby-Spera and Saleeby (1987) as a fault formed during Cretaceous syndepositional caldera collapse. Later mapping (Sisson and Moore, 2013) found no evidence of a fault in this area, and while we observed local evidence of brittle-ductile shearing and steeply plunging lineation, we concur with the interpretation of Sisson and Moore (2013) that the contact is primarily a folded angular unconformity and not a fault.

Structural Interpretation

Geologic mapping and U-Pb zircon dating document major stratigraphic and structural discontinuities throughout the Mineral King pendant. These contacts likely include major fault zones as well as originally depositional unconformities and isoclinal infolds with associated ductile flattening and bedding transposition. Cross sections A-A′ and B-B′ (Fig. 4) illustrate our structural interpretation of the Mineral King pendant and are described in detail in the following sections.

An interpretive map (Fig. 8) and diagrammatic cross sections (Fig. 9) highlight contacts between dated assemblages that we interpret to be major discontinuities. We use the present geometry of these discontinuities to infer major structures capable of producing the observed map pattern. In our interpretation, the northern pendant is dominated by tectonically imbricated fault slivers of diverse ages, whereas the structural pattern in the southern pendant is dominated by kilometer-scale northwest-trending folds.

Downloaded from http://pubs.geoscienceworld.org/gsa/geosphere/article-pdf/20/4/1190/6584248/ges02748.1.pdf
by guest

Cross Section A-A′: Northern Mineral King Pendant

In the northern pendant (Figs. 4A and 9A), the dominant structural pattern is complex imbrication of steeply dipping units of disparate age, with relationships that require significant faulting although evidence for discrete shear zones is generally lacking.

Early Cretaceous volcanic assemblage strata on the western edge of the pendant (map unit Kmrt1) are in contact to the east with both dated Permian strata (Pvt) and marble (Trsc) interpreted as Triassic. This contact is interpreted as a folded angular unconformity. An overprint of distributed ductile shearing is indicated, however, by boudinaged pegmatite veins within the metarhyolite tuff unit (Kmrt1) that have been dismembered and vertically extended into individual porphyroclasts (Fig. 16). These pegmatite porphyroclasts have yielded a U-Pb zircon age of 115 Ma and indicate significant mid-Cretaceous vertical elongation.

To the east and well exposed on the ridge west of Timber Gap, units interpreted as part of the Triassic assemblage are interleaved with Permian strata in possibly folded and faulted relations. A slice of dated mid-Cretaceous andesite (Kma) between interpreted Permian and Triassic units (Psp and Trsa) seems likely fault bounded due to the contrast in age with the adjacent units.

East of Timber Gap, the Early Cretaceous volcanic assemblage is sandwiched between an interpreted Triassic unit (Trsa) and Jurassic metadacite tuff (Jmdt) dated at 185 Ma. The contact is slightly sheared but appears little deformed and is here interpreted as the angular unconformity observed elsewhere at the base of the Early Cretaceous assemblage. To the southeast in the Franklin Creek drainage, the Early Cretaceous volcanic assemblage appears to be folded into an isoclinal syncline, but that structure is poorly expressed to the north and has not been traced to this area.

Continuing east, the quartz diorite of Empire Mountain (Kem) is exposed in a wedge that splits the Jurassic assemblage, suggesting layer-parallel intrusion into the older pendant rocks as a steeply dipping sill. Intrusion of Kem, and subsequently of a narrow dike of diorite (Kmcp), may have been localized along a shear zone exposed to the south in the Monarch Creek drainage. On the eastern side of Empire Mountain, a dated sliver of the Early Cretaceous volcanic assemblage (Kvcs) is in layer-parallel contact with Jurassic metasedimentary and metavolcanic strata to the east.

Cross Section B-B′: Southern Mineral King Pendant

In the southern pendant (Fig. 4B), the map pattern between Vandever Mountain and Florence Peak suggests a series of tight to isoclinal folds involving the Permian, Triassic, and Early Cretaceous assemblages.

A series of northwest-trending folds in an overall synformal structure is well exposed in the Early Cretaceous volcanic assemblage on Vandever Mountain, in steeply dipping contact with older Permian units to the east. We interpret this contact as a folded angular unconformity, with Early Cretaceous rhyolite tuff (Kmrt3) deposited on an eroded surface underlain by previously deformed Permian and Triassic successions.

Mid-Cretaceous contractional deformation resulted in initial tight folding of the Early Cretaceous assemblage and likely increased tightening of pre-existing folds in the Permian and Triassic assemblages. South of Farewell Gap at Bullion Flat, the Cretaceous volcanic assemblage interfingers with Permian strata in a map pattern that is consistent with repeated tight infolds of the Cretaceous volcanic assemblage into the older Permian strata. The volcanic units in this area are undated, however, and therefore other interpretations are possible.

Tight northwest-trending folds are also well exposed in Triassic strata on Tulare Peak and vicinity. The hinge traces of these folds appear to trend into and be cut off by the late Permian–Early Triassic discontinuity on the eastern wall of Farewell Canyon, suggesting that the originally depositional contact was modified by subsequent faulting.

Across the entire pendant, contacts with the bounding mid-Cretaceous plutons of the Sierra Nevada batholith (Kcc and Kcp) are generally sharp and undeformed, with chilled margins and small intrusive veins from the granitic plutons into the country rocks. Narrow zones of ductile to semi-brittle shearing are observed locally, but in general, contacts between pendant rocks and the bounding granitic plutons appear intrusive and tightly bound. There is little evidence for the large-scale relative displacements that would accommodate rapid downward descent of subaerially deposited pendant rocks into contact with mid-crustal plutons.

Dating and Structural Interpretations

Our results in the Mineral King pendant demonstrate that detailed dating is critical for any stratigraphic or structural interpretation of these rocks. A characteristic feature of our work has been that almost all dated samples yielded unexpected results inconsistent with the ages of adjacent units. Dates appear accurate, and repeated dating of the same unit generally yields the same date. The characteristic pattern is more-or-less obscured structural imbrication and transposition of units, at scales ranging from meters to kilometers.

A diagrammatic cross section across the northern pendant emphasizing dated units (Fig. 9A) illustrates this structural pattern. Documented U-Pb zircon ages in this 5-km-long transect are, from west to east: 137 Ma, 277 Ma, 105 Ma, 136 Ma, 185 Ma, 106 Ma (Empire pluton), 136 Ma, and 183 Ma. These dated units are separated by four mapped units interpreted as Late Triassic (ca. 225 Ma) based on correlation to fossiliferous units to the south, and two mapped units interpreted as Jurassic (ca. 200 Ma).

Units are steeply dipping (Fig. 12), with variably developed layer-parallel flattening foliation and steeply plunging stretching lineation, and there are few localized zones of more intense deformation to indicate the presence of major fault zones. Nevertheless, imbrication of narrow (100–500 m) steeply dipping slivers of middle Cretaceous volcanic rocks (e.g., Kma and Kmrd on

Downloaded from http://pubs.geoscienceworld.org/gsa/geosphere/article-pdf/20/4/1190/6584248/ges02748.1.pdf
by guest

Miners Ridge to the south) into Triassic and Jurassic rocks requires large differential displacements most reasonably accommodated by ductile shearing.

DISCUSSION

Mineral King Pendant and the Sierra Nevada Magmatic Arc

Late Permian to mid-Cretaceous rocks of the Mineral King and other wall-rock pendants record the initiation and evolution of the Sierra Nevada magmatic arc on the southwestern margin of Laurentia. The stratigraphic and structural evolution of the Mineral King pendant generally reflects broader regional patterns while providing insight into local arc evolution. Peaks in magmatic activity in Mineral King pendant are, however, different from observed pulses of magmatic activity in the central and eastern Sierra Nevada, suggesting that these "flare-ups" may be more locally variable than previously thought (Sisson and Moore, 2013; Klemetti et al., 2014; Paterson and Ducea, 2015; Cao et al., 2015; Barth et al., 2018; Attia et al., 2022).

In the following sections, we discuss connections between the stratigraphic and structural evolution of the Mineral King pendant and regional evidence for the development of the Sierra Nevada magmatic arc.

Late Permian Assemblage

The basement framework of the southern Sierra Nevada formed initially during a complex series of sinistral truncation events that culminated in late Permian time with initiation of subduction along a northwest-trending Cordilleran continental margin (e.g., Dickinson and Lawton, 2001; Stevens et al., 2005; Saleeby and Dunne, 2015; Clemmons-Knott and Gevedon, 2023). Late Permian magmatism related to arc initiation is documented from the El Paso Mountains (273 ± 4.4 Ma; Cecil et al., 2019), the western Mojave Desert (273 ± 2.4 Ma; Chapman et al., 2012), and the Kern Plateau (273.8 ± 2.3 Ma; Clemens-Knott and Gevedon, 2023).

In the Mineral King pendant, felsic tuff interlayered with siliceous and calc-siliceous hornfels has yielded a U-Pb zircon age of 276.9 ± 1.9 Ma, indicating that Mineral King pendant rocks are recording the earliest inception of magmatic activity in the developing Sierra Nevada arc. The Mineral King pendant is located along the same trend as the Kern Plateau pendants of the El Paso terrane to the southeast, which is characterized by Paleozoic deep-water clastic sediments with interlayered chert (Dunne and Suczek, 1991; Saleeby and Dunne, 2015; Clemens-Knott and Gevedon, 2023). Late Permian strata in Mineral King pendant may have originally been deposited on a basement consisting of Paleozoic El Paso terrane rocks that had previously been transported southward during late Paleozoic sinistral truncation of the Cordilleran margin (Davis et al., 1978; Stone and Stevens, 1988; Saleeby and Dunne, 2015; Clemens-Knott and Gevedon, 2023).

Age Gap 1 (<269–249 Ma: Late Permian to Early Triassic)

Regional contractional and transpressional deformation during latest Permian to Middle Triassic time is recognized on the southwestern Cordilleran margin and attributed to changes from sinistral oblique to more arc-normal subduction (e.g., Snow, 1992; Stevens and Greene, 2000; Stevens and Stone, 2002; Saleeby and Dunne, 2015; Clemens-Knott and Gevedon, 2023).

These events are interpreted to have resulted in uplift and erosion or non-deposition across the Sierra Nevada with development of a Sierra Nevada–wide Permo-Triassic unconformity (Attia et al., 2021). In the Mineral King pendant, this period of regional deformation is likely reflected by non-preservation of strata between ca. 269 Ma and 249 Ma and development of an unconformity between the late Permian and Middle to Late Triassic assemblages.

Middle to Late Triassic Assemblage

From Middle Triassic to early Middle Jurassic time, a lengthy period of slab rollback is proposed to have led to extension across the Sierra Nevada arc and development of a regional submarine arc graben system (Busby-Spera, 1988; Saleeby and Busby, 1993; Saleeby and Dunne, 2015; Clemens-Knott and Gevedon, 2023). By Middle Triassic time, a magmatic arc was well established across the Sierra Nevada region, with deposition from volcanic centers into proximal subaerial and submarine basins (Tobisch et al., 2000; Barth et al., 2011; Attia et al., 2021).

In the Mineral King pendant, protoliths of the Middle Triassic metasandstone turbidites and thin-bedded siliceous and calc-silicate hornfels were deposited, culminating in thick Late Triassic marbles. These marbles may represent a widespread but relatively short-lived carbonate platform suggested to have developed in Late Triassic time across the southern Sierra Nevada region (Saleeby and Busby, 1993; Saleeby and Dunne, 2015).

Age Gap 2 (ca. 218–198 Ma: Late Triassic to Early Jurassic)

A Late Triassic to earliest Jurassic unconformity is proposed to have formed across the Sierra Nevada region concurrent with a reduction in volcanic activity, possibly due to extensional exhumation associated with continuing slab rollback (Saleeby and Dunne, 2015; Attia et al., 2021). In the Mineral King pendant, a hiatus of 18 m.y. between marine sedimentary and intermediate to felsic volcanic rocks of Late Triassic age and calc-siliceous and felsic volcanic rocks of Early Jurassic age may represent this unconformity.

Early Jurassic Assemblage

Synextensional arc volcanism is recorded in Sierran pendants until ca. 190 Ma, followed by a phase of low magmatic flux from 190 Ma to 175 Ma (Saleeby

Downloaded from http://pubs.geoscienceworld.org/gsa/geosphere/article-pdf/20/4/1190/6584248/ges02748.1.pdf
by guest

and Dunne, 2015; Attia et al., 2021). During this low-flux period, extensional exhumation may have led to unconformable deposition of volcanic-poor siliciclastic turbidites on older metamorphic basement. In the Mineral King pendant, thin-bedded siliceous, calc-siliceous, and calcareous strata interlayered with variably reworked felsic volcanic rocks are characteristic of this time period, possibly reflecting deposition in local extensional basins within the arc.

Age Gap 3 (ca. 183–137 Ma: Middle Jurassic to Early Cretaceous)

In late Middle Jurassic time, the flux of arc magmatism accelerated in the Sierra Nevada, with plutonism throughout the Sierran arc (Saleeby and Dunne, 2015). Regional contraction became dominant in Early Cretaceous time (Tobisch et al., 2000; Dunne and Walker, 2004; Cao et al., 2015; Saleeby and Dunne, 2015) coeval with increasing magmatic flux and the beginning of emplacement of the Cretaceous Sierra Nevada batholith at ca. 140 Ma. These events resulted in the development of a Late Jurassic–Early Cretaceous unconformity recognized across much of the Sierra Nevada (Attia et al., 2021).

The Mineral King pendant in Middle and Late Jurassic time is characterized by non-deposition between 183 Ma and ca. 135 Ma. Hornblende gabbro bodies were intruded at 183 Ma and 162 Ma, but no sedimentary or volcanic strata of Middle to Late Jurassic age have been documented. Deformation, uplift, and erosion during this period produced a prominent erosion surface underlain by deformed Permo-Triassic and Early Jurassic rocks.

Early Cretaceous Assemblage

Across much of the central and southern Sierra Nevada, Cretaceous strata are deposited above a major Jurassic to Early Cretaceous angular unconformity (Attia et al., 2021). Magmatic activity in the Sierra Nevada arc was rare between 140 Ma and 120 Ma, reflecting a magmatic lull that preceded the mid-Cretaceous "flare-up" of voluminous plutonism and associated volcanism (Paterson and Ducea, 2015; Cao et al., 2015; Attia et al., 2022). Felsic magmatism of this age is, however, preserved in the Mount Goddard and western Ritter Range pendants in the central Sierra Nevada (Tobisch et al., 1986; Fiske and Tobisch, 1994).

In the Mineral King pendant, distinctive voluminous rhyolite tuffs were erupted in a major event between 137 Ma and 134 Ma, accompanied by emplacement of the granodiorite of White Chief Mine at 135 Ma. Two plutons south and west of Mineral King pendant were also emplaced during this time: the granodiorite of Camelback Ridge (133 ± 1 Ma) and the granodiorite of Burnt Camp Creek (134.8 ± 1.5 Ma) (Sisson and Moore, 2013). All three of these granodiorite plutons are sheared and strongly foliated, in contrast to younger plutons in and adjacent to the pendant.

Age Gap 4 (ca. 134 Ma to ≤118 Ma: Mid-Cretaceous)

The final flare-up of the Sierran arc began at ca. 125 Ma (Paterson and Ducea, 2015; Attia et al., 2020, 2022). Intra-arc strata from this period are generally poorly preserved, possibly due to predominantly subaerial deposition on upland surfaces. In the Mineral King pendant, there is a distinct hiatus between deposition of the rhyolite tuffs at ca. 135 Ma and that of mixed felsic volcanic and reworked volcaniclastic rocks deposited beginning at ca. 118 Ma.

Middle Cretaceous Assemblage

Plutonism in the Sierra Nevada batholith peaked between 100 Ma and 85 Ma with the emplacement of the large Tuolumne, John Muir, and Mount Whitney Intrusive Suites along the axis of the range (Hirt, 2007; Davis et al., 2012; Memeti et al., 2022). Mid-Cretaceous contractional and later transpressional deformation coeval with pluton emplacement is widely recorded (e.g., Greene and Schweickert, 1995; Tikoff and de Saint Blanquat, 1997; Sharp et al., 2000; Tobisch et al., 2000; Cao et al., 2016; Krueger and Yoshinobu, 2018; Attia et al., 2022).

In the Mineral King pendant, a major magmatic phase began ca. 110 Ma with intrusion of the quartz diorite of Empire Mountain at 106 Ma and the granodiorite of Spring Lake at 104 Ma. Felsic volcanic tuffs were deposited at 105–101 Ma, and the large bounding plutons of the granite of Coyote Pass (99 Ma) and the granodiorite of Castle Creek (98 Ma) were emplaced (Sisson and Moore, 2013).

Major mid-Cretaceous contractional deformation associated with this phase in the Mineral King pendant is indicated by: (1) tight kilometer-scale folding of Early Cretaceous 135 Ma volcanic strata and the underlying unconformity surface; (2) tilting of 101 Ma felsic volcanic strata to vertical dips and structural interleaving with older strata; (3) development of strong flattening foliation and down-dip stretching lineation in all units including 101 Ma volcanic strata; and (4) sheared and boudinaged pegmatite veins dated at 115 Ma, and folded aplite dikes dated at 98 Ma (Sisson and Moore, 2013).

This phase of imbrication, tilting, flattening, and vertical elongation coincided with the emplacement of the sill-like quartz diorite of Empire Mountain into the pendant and was coeval with or immediately followed by the emplacement of the large bounding plutons that define the present shape of the Mineral King pendant.

Mid-Cretaceous Deformation in Mineral King Pendant and the Western U.S. Cordillera

Our work demonstrates that a major mid-Cretaceous deformational event occurred in the Mineral King pendant during a narrow window of time between

Downloaded from http://pubs.geoscienceworld.org/gsa/geosphere/article-pdf/20/4/1190/6584248/ges02748.1.pdf
by guest

ca. 115 Ma and 98 Ma. Both the large-scale structural geometry and the dominant deformational fabric in the pendant were established at this time. At least one earlier phase of deformation is indicated by the juxtaposition of contrasting Permian and Triassic units that underlie the Early Cretaceous angular unconformity, but discrete structures from this time period are obscure, and the lack of an early ductile fabric suggests predominantly upper crustal deformation. Because almost all structures in the pendant involve well-dated units ranging in age from 135 Ma to 101 Ma, the predominant structural architecture and bulk of the deformation must have formed during this short period in the mid-Cretaceous.

Complex imbrication of pendant strata along multiple, vertically dipping, parallel to anastomosing fault zones are required by our U-Pb dating results. Volcanosedimentary strata as young as 101 Ma are vertically dipping and imbricated with Triassic and Jurassic units, indicating substantial mid-Cretaceous offsets on the now-cryptic bounding faults. Northwest-striking, steeply dipping flattening foliation and steeply plunging stretching lineation are variably developed but pervasive throughout the pendant. This pattern of deformation is characteristic of pure-shear dominated transpression (e.g., Fossen and Tikoff, 1993, 1998; Tikoff and Greene, 1997).

There is increasing evidence for a major phase of contractional to dextral transpressional deformation in the western U.S. Cordillera between ca. 100 Ma and 85 Ma (e.g., Hildebrand and Whalen, 2021; Tikoff et al., 2023). In the Sierra Nevada, mid-Cretaceous contractional and dextral transpressional deformation beginning ca. 100 Ma has been previously documented in numerous, although mostly localized, shear zones including the proto–Kern Canyon shear zone (Nadin and Saleeby, 2008), the Courtright-Wishon shear zone (Tobisch et al., 1995; Torres Andrade and Tikoff, 2022), the Sing Peak shear zone (Krueger and Yoshinobu, 2018), the Bench Canyon shear zone (McNulty, 1995), the Rosy Finch shear zone (Tikoff and de Saint Blanquat, 1997), the Gem Lake shear zone (Greene and Schweickert, 1995), and the Cascade Lake shear zone (Tikoff et al., 2005; Cao et al., 2015). Structures indicating mid-Cretaceous contraction and dextral transpression between ca. 100 Ma and 85 Ma are also well developed in Cretaceous plutons in northwestern Nevada (e.g., Wyld and Wright, 2001; Trevino and Tikoff, 2023) and in the Idaho batholith (e.g., Giorgis et al., 2008; Braudy et al., 2017). A tectonic model involving oblique collision of the Insular superterrane with the margin of North America between 100 Ma and 85 Ma (the "hit-and-run model") has been proposed to explain this widespread orogenic event (Maxson and Tikoff, 1996; Tikoff et al., 2023). Mid-Cretaceous transpressional deformation in the Mineral King pendant as documented herein provides significant new evidence supporting a mid-Cretaceous transpressional orogenic event in the western U.S. Cordillera.

CONCLUSIONS

Revision of the geologic map of the Mineral King pendant, to emphasize age relationships and structures documented by U-Pb dating rather than lithologic or stratigraphic correlations, allows a more coherent interpretation of geologic events in the pendant. Many uncertainties remain for future work, however.

Pendant rocks are structurally imbricated by a combination of kilometer-scale tight to isoclinal folding and cryptic faulting, accentuated by, and eventually obscured by, pervasive flattening and vertical stretching that preceded and accompanied emplacement of the bounding mid-Cretaceous plutons. These observations preclude previous interpretations of an east-facing homocline.

There is little direct evidence for discrete faults or ductile shear zones in the Mineral King pendant, although such structures are necessary to produce the structural imbrications revealed by our new mapping and U-Pb dating. Pervasive ductile deformation including steeply dipping flattening foliation, steeply plunging stretching lineation, and complex imbrication of volcanosedimentary strata and associated intrusions as young as 101 Ma add to growing evidence of major transpressional tectonism in the Sierra Nevada and western Cordillera between 100 Ma and 85 Ma.

Much of the stratigraphic and structural complexity in the Mineral King pendant is identifiable only through detailed dating and the fortuitous presence of a distinctive stratigraphic marker that allows identification of tight kilometer-scale folds. Detailed dating in other Sierran pendants will likely also indicate much more complex structural histories than are presently documented.

We identify five tectonostratigraphic assemblages ranging from middle Permian to mid-Cretaceous in age, and four significant structural and/or stratigraphic breaks that allow us to interpret the following geologic history for the Mineral King pendant:

(1) Deposition of late Permian, primarily marine sedimentary and interbedded felsic volcanic and volcanosedimentary rocks, 277 Ma to ca. 269 Ma.
(2) Early Triassic depositional hiatus, ca. 269–249 Ma.
(3) Deposition of Middle to Late Triassic marine strata, including fine-grained siliceous and calc-silicate rocks, bedded carbonates, and andesitic and felsic volcanics, 249–218 Ma.
(4) Possible Early Jurassic depositional hiatus, 218–198 Ma.
(5) Deposition of Early Jurassic siliceous and calc-siliceous marine strata interbedded with felsic volcanic and volcaniclastic strata, 198–183 Ma.
(6) Depositional hiatus, 183–137 Ma. Fold-thrust(?) deformation, imbrication, uplift, and erosion.
(7) Subaerial to shallow marine deposition of voluminous rhyolite ash-flow tuffs, variably reworked in a shallow marine environment, deposited in angular unconformity on previously deformed older units, 137–134 Ma. Emplacement of White Chief pluton at 135 Ma.
(8) Mid-Cretaceous depositional hiatus, 134 Ma to ca. 118 Ma.
(9) Subaerial to shallow marine deposition of variably reworked felsic volcanic rocks and volcanogenic sandstones, ca. 118 Ma to 101 Ma. Emplacement of the Empire Mountain pluton at ~3.3 km depth at 106 Ma (D'Errico et al., 2012).

Downloaded from http://pubs.geoscienceworld.org/gsa/geosphere/article-pdf/20/4/1190/6584248/ges02748.1.pdf
by guest

(10) Episodic contractional deformation, including tilting, flattening, and vertical extension as indicated by steeply dipping rhyolite tuffs with ages ranging from 105 Ma to 101 Ma, extensively boudinaged pegmatite dikes dated at 115 Ma, and isoclinally folded aplite dikes dated at 98 Ma (Sisson and Moore, 2013).

(11) Intrusion of bounding Castle Creek and Coyote Pass plutons (99–98 Ma), synchronous with the last phase of contractional deformation. Close juxtaposition of supracrustal rhyolite tuffs deposited at ca. 100 Ma and large granitic plutons crystalized at ~11 km depth indicating rapid downward displacement of wall rocks synchronous with pluton emplacement.

ACKNOWLEDGMENTS

We thank Tom Sisson, Charles Hoffman, Conner Toth, Nathan Thorne, Cory Van Auken, and Thom Worm for enlightening discussions and assistance with field work; Judith Greene-Janse for assistance with graphics; and the National Park Service for permitting sampling for this project. Helpful reviews by Basil Tikoff, Tom Sisson, and Terry Pavlis substantially improved the final paper. Funding support was provided by the Anderson Scholars program at Denison University and the Denison University Research Fund. Lackey is supported by U.S. National Science Foundation grants EAR-0948706 and OCE-1338842. Geochronology in the Oxtoby Isotope Laboratory at Pomona College is funded in large part by the Gordon and Betty Moore Foundation (GMBF-5417).

REFERENCES CITED

Allmendinger, R.W., Cardozo, N., and Fisher, D.M., 2012, Structural Geology Algorithms: Vectors and Tensors: Cambridge, UK, Cambridge University Press, 289 p.

Ardill, K., Memeti, V., and Paterson, S., 2020, Reconstructing the physical and chemical development of a pluton-porphyry complex in a tectonically reorganized arc crustal section, Tioga Pass, Sierra Nevada: Lithosphere, v. 2020, https://doi.org/10.2113/2020/8872875.

Attia, S., Paterson, S.R., Cao, W., Chapman, A.D., Saleeby, J., Dunne, G.C., Stevens, C.H., and Memeti, V., 2018, Late Paleozoic tectonic assembly of the Sierra Nevada prebatholithic framework and western Laurentian provenance links based on synthesized detrital zircon geochronology, *in* Ingersoll, R.V., Lawton, T.F., and Graham, S.A., eds., Tectonics, Sedimentary Basins, and Provenance: A Celebration of William R. Dickinson's Career: Geological Society of America Special Paper 540, p. 267–295, https://doi.org/10.1130/2018.2540(12).

Attia, S., Cottle, J.M., and Paterson, S.R., 2020, The erupted zircon record of continental crust formation during mantle driven arc flare-ups: Geology, v. 48, p. 446–451, https://doi.org/10.1130/G46991.1.

Attia, S., Paterson, S.R., Saleeby, J., and Cao, W., 2021, Detrital zircon provenance and depositional links of Mesozoic Sierra Nevada intra-arc strata: Geosphere, v. 17, p. 1422–1453, https://doi.org/10.1130/GES02296.1.

Attia, S., Paterson, S.R., Jiang, D., and Miller, R.B., 2022, Spatiotemporally heterogeneous deformation, indirect tectonomagmatic links, and lithospheric evolution during orogenic activity coeval with an arc flare-up: Geosphere, v. 18, p. 1752–1782, https://doi.org/10.1130/GES02478.1.

Barth, A.P., Walker, J.D., Wooden, J.L., Riggs, N.R., and Schweickert, R.A., 2011, Birth of the Sierra Nevada magmatic arc: Early Mesozoic plutonism and volcanism in the east-central Sierra Nevada of California: Geosphere, v. 7, p. 877–897, https://doi.org/10.1130/GES00661.1.

Barth, A.P., Wooden, J.L., Riggs, N.R., Walker, J.D., Tani, K., Penniston-Dorland, S.C., Jacobson, C.E., Laughlin, J.A., and Hiramatsu, R., 2018, Marine volcaniclastic record of early arc evolution in the eastern Ritter Range pendant, central Sierra Nevada, California: Geochemistry, Geophysics, Geosystems, v. 19, p. 2543–2559, https://doi.org/10.1029/2018GC007456.

Bateman, P.C., and Wahrhaftig, C., 1966, Geology of the Sierra Nevada, *in* Bailey, E.H., ed., Geology of Northern California: California Division of Mines and Geology Bulletin 190, p. 107–172.

Braudy, N., Gaschnig, R.M., Wilford, D., Vervoort, J.D., Nelson, C.L., Davidson, C., Kahn, M.J., and Tikoff, B., 2017, Timing and deformation conditions of the western Idaho shear zone, West Mountain, west-central Idaho: Lithosphere, v. 9, p. 157–183, https://doi.org/10.1130/L519.1.

Busby-Spera, C.J., 1983, Paleogeographic reconstruction of a submarine volcanic center: geochronology, volcanology and sedimentology of the Mineral King roof pendant, Sierra Nevada, California [Ph.D. thesis]: Princeton, New Jersey, Princeton University, 317 p.

Busby-Spera, C.J., 1984, Large-volume rhyolite ash flow eruptions and submarine caldera collapse in the Lower Mesozoic Sierra Nevada, California: Journal of Geophysical Research: Solid Earth, v. 89, p. 8417–8427, https://doi.org/10.1029/JB089iB10p08417.

Busby-Spera, C.J., 1985, A sand-rich submarine fan in the lower Mesozoic Mineral King caldera complex, Sierra Nevada, California: Journal of Sedimentary Petrology, v. 55, p. 376–391, https://doi.org/10.1306/212F86D9-2B24-11D7-8648000102C1865D.

Busby-Spera, C.J., 1986, Depositional features of rhyolitic and andesitic volcaniclastic rocks of the Mineral King submarine caldera complex, Sierra Nevada, California: Journal of Volcanology and Geothermal Research, v. 27, p. 43–76, https://doi.org/10.1016/0377-0273(86)90080-6.

Busby-Spera, C.J., 1988, Speculative tectonic model for the lower Mesozoic arc of the southwest Cordilleran United States: Geology, v. 16, p. 1121–1125, https://doi.org/10.1130/0091-7613(1988)016<1121:STMFTE>2.3.CO;2.

Busby-Spera, C.J., and Saleeby, J., 1987, Geologic guide to the Mineral King area, Sequoia National Park, California: Pacific Section, Society of Economic Paleontologists and Mineralogists Guidebook 56, 44 p.

Cao, W., Paterson, S.R., Memeti, V., Mundil, R., Anderson, J.L., and Schmidt, K., 2015, Tracking paleodeformation fields in the Mesozoic central Sierra Nevada arc: Implications for intra-arc cyclic deformation and arc tempos: Lithosphere, v. 7, p. 296–320, https://doi.org/10.1130/L389.1.

Cao, W., Paterson, S.R., Saleeby, J., and Zalunardo, S., 2016, Bulk arc strain, crustal thickening, magma emplacement, and mass balances in the Mesozoic Sierra Nevada arc: Journal of Structural Geology, v. 84, p. 14–30, https://doi.org/10.1016/j.jsg.2015.11.002.

Cardozo, N., and Allmendinger, R.W., 2013, Spherical projections with OSXStereonet: Computers & Geosciences, v. 51, p. 193–205, https://doi.org/10.1016/j.cageo.2012.07.021.

Cecil, M.R., Ferrer, M.A., Riggs, N.R., Marsaglia, K., Kylander-Clark, A., Ducea, M.N., and Stone, P., 2019, Early arc development recorded in Permian–Triassic plutons of the northern Mojave Desert region, California, USA: Geological Society of America Bulletin, v. 131, p. 749–765, https://doi.org/10.1130/B31963.1.

Chapman, A.D., Saleeby, J.B., Wood, D.J., Piasecki, A., Kidder, S., Ducea, M.N., and Farley, K.A., 2012, Late Cretaceous gravitational collapse of the southern Sierra Nevada batholith, California: Geosphere, v. 8, p. 314–341, https://doi.org/10.1130/GES00740.1.

Chapman, A.D., Ernst, W.G., Gottlieb, E., Powerman, V., and Metzger, E.P., 2015, Detrital zircon geochronology of Neoproterozoic–Lower Cambrian passive-margin strata of the White-Inyo Range, east-central California: Implications for the Mojave–Snow Lake fault hypothesis: Geological Society of America Bulletin, v. 127, p. 926–944, https://doi.org/10.1130/B31142.1.

Christensen, M.N., 1959, Geologic structure of the Mineral King area, California [Ph.D. thesis]: Berkeley, University of California, Berkeley, 102 p.

Christensen, M.N., 1963, Structure of metamorphic rocks at Mineral King, California: University of California Publications in Geological Sciences, v. 42, p. 159–198.

Clemens-Knott, D., and Gevedon, M., 2023, Using discordant U-Pb zircon data to re-evaluate the El Paso terrane: Late Paleozoic tectonomagmatic evolution of east-central California (USA) and intense hydrothermal activity in the Jurassic Sierra Nevada arc: Geosphere, v. 19, p. 531–557, https://doi.org/10.1130/GES02547.1.

Davis, G.A., Monger, J.W.H., and Burchfiel, B.C., 1978, Mesozoic construction of the Cordilleran "collage", central British Columbia to central California, *in* Howell, D.G., and McDougall, K.A., eds., Mesozoic Paleogeography of the Western United States: Pacific Section, Society of Economic Paleontologists and Mineralogists Pacific Coast Paleogeography Symposium 2, p. 1–32.

Davis, J.W., Coleman, D.S., Gracely, J.T., Gaschnig, R., and Stearns, M., 2012, Magma accumulation rates and thermal histories of plutons of the Sierra Nevada batholith, CA: Contributions to Mineralogy and Petrology, v. 163, p. 449–465, https://doi.org/10.1007/s00410-011-0683-7.

D'Errico, M.E., Lackey, J.S., Surpless, B.E., Loewy, S.L., Wooden, J.L., Barnes, J.D., Strickland, A., and Valley, J.W., 2012, A detailed record of shallow hydrothermal fluid flow in the Sierra Nevada magmatic arc from low-^{18}O skarn garnets: Geology, v. 40, p. 763–766, https://doi.org/10.1130/G33008.1.

Dickinson, W.R., and Lawton, T.F., 2001, Carboniferous to Cretaceous assembly and fragmentation of Mexico: Geological Society of America Bulletin, v. 113, p. 1142–1160, https://doi.org/10.1130/0016-7606(2001)113<1142:CTCAAF>2.0.CO;2.

Downloaded from http://pubs.geoscienceworld.org/gsa/geosphere/article-pdf/20/4/1190/6584248/ges02748.1.pdf
by guest

Dunne, G.C., and Suczek, C.A., 1991, Early Paleozoic eugeoclinal strata in the Kern Plateau pendants, southern Sierra Nevada, California, *in* Cooper, J.D., and Stevens, C.H., eds., Paleozoic Paleogeography of the Western United States: Pacific Section, SEPM (Society for Sedimentary Geology) Special Publication 67, p. 677–692.

Dunne, G.C., and Walker, J.D., 2004, Structure and evolution of the East Sierran thrust system, east central California: Tectonics, v. 23, TC4012, https://doi.org/10.1029/2002TC001478.

Durrell, C., 1940, Metamorphism in the southern Sierra Nevada northeast of Visalia, California: University of California Publications in Geological Sciences, v. 24, p. 1–118.

Fiske, R.S., and Tobisch, O.T., 1978, Paleogeographic significance of volcanic rocks of the Ritter Range pendant, central Sierra Nevada, California, *in* Howell, D.G., and McDougall, K.A., eds., Mesozoic Paleogeography of the Western United States: Pacific Section, Society of Economic Paleontologists and Mineralogists Pacific Coast Paleogeography Symposium 2, p. 209–222.

Fiske, R.S., and Tobisch, O.T., 1994, Middle Cretaceous ash-flow tuff and caldera-collapse deposit in the Minarets Caldera, east-central Sierra Nevada, California: Geological Society of America Bulletin, v. 106, p. 582–593, https://doi.org/10.1130/0016-7606(1994)106<0582:MCAFTA>2.3.CO;2.

Fossen, H., and Tikoff, B., 1993, The deformation matrix for simultaneous simple shearing, pure shearing and volume change, and its application to transpression-transtension tectonics: Journal of Structural Geology, v. 15, p. 413–422, https://doi.org/10.1016/0191-8141(93)90137-Y.

Fossen, H., and Tikoff, B., 1998, Extended models of transpression and transtension, and application to tectonic settings, *in* Holdsworth, R.E., Strachan, R.A., and Dewey, J.F., eds., Continental Transpressional and Transtensional Tectonics: Geological Society of London Special Publication 135, p. 15–33, https://doi.org/10.1144/GSL.SP.1998.135.01.02.

Gehrels, G.E., 2014, Detrital zircon U-Pb geochronology applied to tectonics: Annual Review of Earth and Planetary Sciences, v. 42, p. 127–149, https://doi.org/10.1146/annurev-earth-050212-124012.

Giorgis, S., McClelland, W., Fayon, A., Singer, B.S., and Tikoff, B., 2008, Timing of deformation and exhumation in the western Idaho shear zone, McCall, Idaho: Geological Society of America Bulletin, v. 120, p. 1119–1133, https://doi.org/10.1130/B26291.1.

Goodwin, J.G., 1958, Mines and mineral resources of Tulare County, California: California Journal of Mines and Geology, v. 54, p. 317–492.

Goodyear, W.A., 1888, Tulare County, *in* Irelan, W., Jr., ed., Eighth Annual Report of the State Mineralogist for the Year Ending October 1, 1888: Sacramento, California State Mining Bureau, p. 643–652.

Greene, D.C., and Schweickert, R.A., 1995, The Gem Lake shear zone: Cretaceous dextral transpression in the Northern Ritter Range pendant, eastern Sierra Nevada, California: Tectonics, v. 14, p. 945–961, https://doi.org/10.1029/95TC01509.

Greene, D.C., and Stevens, C.H., 2002, Geologic map of Paleozoic rocks in the Mount Morrison pendant, eastern Sierra Nevada, California: California Division of Mines and Geology Map Sheet 53, 1:24000.

Greene, D.C., Schweickert, R.A., and Stevens, C.H., 1997, Roberts Mountains allochthon and the western margin of the Cordilleran miogeocline in the Northern Ritter Range pendant, eastern Sierra Nevada, California: Geological Society of America Bulletin, v. 109, p. 1294–1305, https://doi.org/10.1130/0016-7606(1997)109<1294:RMAATW>2.3.CO;2.

Greene, D.C., Hoffman, C.F., and Lackey, J.S., 2020, Complexly interleaved Permian to mid-Cretaceous volcano-sedimentary rocks in the Mineral King pendant, southern Sierra Nevada, California indicate multiple deformations prior to and synchronous with Cretaceous batholith emplacement: Geological Society of America Abstracts with Programs, v. 52, no. 4, https://doi.org/10.1130/abs/2020CD-347021.

Hildebrand, R.S., and Whalen, J.B., 2021, The mid-Cretaceous Peninsular Ranges orogeny: A new slant on Cordilleran tectonics? I: Mexico to Nevada: Canadian Journal of Earth Sciences, v. 58, p. 670–696, https://doi.org/10.1139/cjes-2020-0154.

Hirt, W.H., 2007, Petrology of the Mount Whitney Intrusive Suite, eastern Sierra Nevada, California: Implications for the emplacement and differentiation of composite felsic intrusions: Geological Society of America Bulletin, v. 119, p. 1185–1200, https://doi.org/10.1130/B26054.1.

Hoffman, C.F., Greene, D.C., Klemetti, E.W., Toth, C., and Worm, T.J., 2017, Compilation of new and existing age data indicates large scale structural imbrication in the Mineral King pendant, southern Sierra Nevada, California: Geological Society of America Abstracts with Programs, v. 49, no. 6, https://doi.org/10.1130/abs/2017AM-300026.

Jennings, C.W., 1977, Geologic map of California: Sacramento, California Division of Mines and Geology California Geologic Data Map 2, scale 1:750,000.

Kistler, R.W., 1990, Two different lithosphere types in the Sierra Nevada, California, *in* Anderson, J.L., ed., The Nature and Origin of Cordilleran Magmatism: Geological Society of America Memoir 174, p. 271–282, https://doi.org/10.1130/MEM174-p271.

Kistler, R.W., 1993, Mesozoic intrabatholithic faulting, Sierra Nevada, California, *in* Dunne, G.C., and McDougall, K.A., eds., Mesozoic Paleogeography of the Western United States—II: Pacific Section, SEPM (Society for Sedimentary Geology) Book 71, p. 247–259.

Klemetti, E.W., Williamson, A.L., Greene, D.C., and Lackey, J.S., 2013, Geothermobarometry of the Castle Creek quartz monzodiorite supports rapid Cretaceous subsidence of the Mineral King metamorphic pendant, Sierra Nevada, California: Geological Society of America Abstracts with Programs, v. 45, no. 7, p. 610.

Klemetti, E.W., Lackey, J.S., and Starnes, J., 2014, Magmatic lulls in the Sierra Nevada captured in zircon from rhyolite of the Mineral King pendant, California: Geosphere, v. 10, p. 66–79, https://doi.org/10.1130/GES00920.1.

Knopf, A., and Thelan, P., 1905, Sketch of the geology of Mineral King, California: University of California Publications Bulletin of the Department of Geology, v. 4, no. 12, p. 227–262.

Krueger, R.J., and Yoshinobu, A.S., 2018, Structures in the Jackass Lakes pluton–host-rock system, central Sierra Nevada, California, and inferred mid-Cretaceous Farallon–North America plate kinematics: Geological Society of America Bulletin, v. 130, p. 1940–1958, https://doi.org/10.1130/B31992.1.

Maxson, J., and Tikoff, B., 1996, A hit-and-run model for the Laramide orogeny, western United States: Geology, v. 24, p. 968–972, https://doi.org/10.1130/0091-7613(1996)024<0968:HARCMF>2.3.CO;2.

McNulty, B.A., 1995, Shear zone development during magmatic arc construction: The Bench Canyon shear zone, central Sierra Nevada, California: Geological Society of America Bulletin, v. 107, p. 1094–1107, https://doi.org/10.1130/0016-7606(1995)107<1094:SZDDMA>2.3.CO;2.

Memeti, V., Gehrels, G.E., Paterson, S.R., Thompson, J.M., Mueller, R.M., and Pignotta, G.S., 2010, Evaluating the Mojave–Snow Lake fault hypothesis and origins of central Sierran metasedimentary pendant strata using detrital zircon provenance analyses: Lithosphere, v. 2, p. 341–360, https://doi.org/10.1130/L58.1.

Memeti, V., Paterson, S.R., and Mundil, R., 2022, Coupled magmatic and host rock processes during the initiation of the Tuolumne Intrusive Complex: A transition from ephemeral sheets to long-lived, active magma mushes: Geological Society of America Bulletin, v. 134, p. 1347–1374, https://doi.org/10.1130/B35871.1.

Nadin, E.S., and Saleeby, J.B., 2008, Disruption of regional primary structure of the Sierra Nevada batholith by the Kern Canyon fault system, California, *in* Wright, J.E., and Shervais, J.W., eds., Ophiolites, Arcs, and Batholiths: A Tribute to Cliff Hopson: Geological Society of America Special Paper 438, p. 429–454, https://doi.org/10.1130/2008.2438(15).

Nadin, E.S., Saleeby, J., and Wong, M., 2016, Thermal evolution of the Sierra Nevada batholith, California, and implications for strain localization: Geosphere, v. 12, p. 377–399, https://doi.org/10.1130/GES01224.1.

Nokleberg, W.J., 1983, Wallrocks of the central Sierra Nevada batholith, California: A collage of accreted tectono-stratigraphic terranes: U.S. Geological Survey Professional Paper 1255, 28 p., https://doi.org/10.3133/pp1255.

Paterson, S.R., and Ducea, M.N., 2015, Arc magmatic tempos: Gathering the evidence: Elements, v. 11, p. 91–98, https://doi.org/10.2113/gselements.11.2.91.

Paterson, S.R., and Memeti, V., 2014, Mesozoic volcanic rocks of the central Sierra Nevada arc, *in* Memeti, V., Paterson, S.R., and Putirka, K.D., eds., Formation of the Sierra Nevada Batholith: Magmatic and Tectonic Processes and Their Tempos: Geological Society of America Field Guide 34, p. 75–85, https://doi.org/10.1130/2014.0034(05).

Ryan-Davis, J., Lackey, J.S., Gevedon, M., Barnes, J.D., Lee, C.-T.A., Kitajima, K., and Valley, J.W., 2019, Andradite skarn garnet records of exceptionally low $\delta^{18}O$ values within an Early Cretaceous hydrothermal system, Sierra Nevada, CA: Contributions to Mineralogy and Petrology, v. 174, 68, https://doi.org/10.1007/s00410-019-1602-6.

Saleeby, J., and Dunne, G., 2015, Temporal and tectonic relations of early Mesozoic arc magmatism, southern Sierra Nevada, California, *in* Anderson, T.H., Didenko, A.N., Johnson, C.L., Khanchuk, A.I., and MacDonald, J.H., Jr., eds., Late Jurassic Margin of Laurasia—A Record of Faulting Accommodating Plate Rotation: Geological Society of America Special Paper 513, p. 223–268, https://doi.org/10.1130/2015.2513(05).

Saleeby, J.B., 1990, Progress in tectonic and petrogenetic studies in an exposed cross-section of young (~100 Ma) continental crust, southern Sierra Nevada, California, *in* Salisbury M.H., ed., Exposed Cross-Sections of the Continental Crust: Norwell, Massachusetts, D. Reidel, p. 137–158, https://doi.org/10.1007/978-94-009-0675-4_6.

Saleeby, J.B., and Busby, C., 1993, Paleogeographic and tectonic setting of axial and western metamorphic framework rocks of the southern Sierra Nevada, California, *in* Dunne, G.C., and McDougall, K.A., eds., Mesozoic Paleogeography of the Western United States—II: Pacific Section, SEPM (Society for Sedimentary Geology) Book 71, p. 197–225.

Downloaded from http://pubs.geoscienceworld.org/gsa/geosphere/article-pdf/20/4/1190/6584248/ges02748.1.pdf
by guest

Saleeby, J.B., Kistler, R.W., Longiaru, S.J., Moore, J.G., and Nokleberg, W.J., 1990, Middle Cretaceous silicic metavolcanic rocks in the Kings Canyon area, central Sierra Nevada, California, *in* Anderson, J.L., ed., The Nature and Origin of Cordilleran Magmatism: Geological Society of America Memoir 174, p. 251–271, https://doi.org/10.1130/MEM174-p251.

Schweickert, R.A., and Lahren, M.M., 1990, Speculative reconstruction of a major Early Cretaceous(?) dextral fault zone in the Sierra Nevada: Implications for Paleozoic and Mesozoic orogenesis in the western United States: Tectonics, v. 9, p. 1609–1629, https://doi.org/10.1029/TC009i006p01609.

Schweickert, R.A., and Lahren, M.M., 1991, Age and significance of metamorphic rocks along the axis of the Sierra Nevada batholith: A critical reappraisal, *in* Cooper, J.D., and Stevens, C.H., eds., Paleozoic Paleogeography of the Western United States—II: Pacific Section, SEPM (Society for Sedimentary Geology) Special Publication 67, p. 653–676.

Schweickert, R.A., and Lahren, M.M., 1993, Triassic–Jurassic magmatic arc in eastern California and western Nevada: Arc evolution, cryptic tectonic breaks and significance of the Mojave–Snow Lake fault, *in* Dunne, G.C., and McDougall, K.A., eds., Mesozoic Paleogeography of the Western United States—II: Pacific Section, SEPM (Society for Sedimentary Geologists) Book 71, p. 227–246.

Sharp, W.D., Tobisch, O.T., and Renne, P.R., 2000, Development of Cretaceous transpressional cleavage synchronous with batholith emplacement, central Sierra Nevada, California: Geological Society of America Bulletin, v. 112, p. 1059–1066, https://doi.org/10.1130/0016-7606(2000)112<1059:DOCTCS>2.0.CO;2.

Sisson, T.W., and Moore, J.G., 2013, Geologic map of southwestern Sequoia National Park, Tulare County, California: U.S. Geological Survey Open-File Report 2013-1096, 26 p., 2 sheets, scale 1:24,000, https://doi.org/10.3133/ofr20131096.

Smith, J.P., 1927, Upper Triassic marine invertebrate faunas of North America: U.S. Geological Survey Professional Paper 141, 262 p., https://doi.org/10.3133/pp141.

Snow, J.K., 1992, Large-magnitude Permian shortening and continental-margin tectonics in the southern Cordillera: Geological Society of America Bulletin, v. 104, p. 80–105, https://doi.org/10.1130/0016-7606(1992)104<0080:LMPSAC>2.3.CO;2.

Stevens, C.H., and Greene, D.C., 1999, Stratigraphy, depositional history, and tectonic evolution of Paleozoic continental-margin rocks in roof pendants of the eastern Sierra Nevada, California: Geological Society of America Bulletin, v. 111, p. 919–933, https://doi.org/10.1130/0016-7606(1999)111<0919:SDHATE>2.3.CO;2.

Stevens, C.H., and Greene, D.C., 2000, Geology of Paleozoic rocks in eastern Sierra Nevada roof pendants, California, *in* Lageson, D.R., Peters, S.G., and Lahren, M.M., eds., Great Basin and Sierra Nevada: Geological Society of America Field Guide 2, p. 237–254, https://doi.org/10.1130/0-8137-0002-7.237.

Stevens, C.H., and Stone, P., 2002, Correlation of Permian and Triassic deformations in the western Great Basin and eastern Sierra Nevada: Evidence from the northern Inyo Mountains near Tinemaha Reservoir, east-central California: Geological Society of America Bulletin, v. 114, p. 1210–1221, https://doi.org/10.1130/0016-7606(2002)114<1210:COPATD>2.0.CO;2.

Stevens, C.H., Stone, P., and Miller, J.S., 2005, A new reconstruction of the Paleozoic continental margin of southwestern North America: Implications for the nature and timing of continental truncation and the possible role of the Mojave-Sonora megashear, *in* Anderson, T.H., Nourse, J.A., McKee, J.W., and Steiner, M.B., eds., The Mojave-Sonora Megashear Hypothesis: Development, Assessment, and Alternatives: Geological Society of America Special Paper 393, p. 597–618, https://doi.org/10.1130/0-8137-2393-0.597.

Stone, P., and Stevens, C.H., 1988, Pennsylvanian and Early Permian paleogeography of east-central California: Implications for the shape of the continental margin and the timing of continental truncation: Geology, v. 16, p. 330–333, https://doi.org/10.1130/0091-7613(1988)016<0330:PAEPPO>2.3.CO;2.

Tikoff, B., and de Saint Blanquat, M., 1997, Transpressional shearing and strike-slip partitioning in the Late Cretaceous Sierra Nevada magmatic arc, California: Tectonics, v. 16, p. 442–459, https://doi.org/10.1029/97TC00720.

Tikoff, B., and Greene, D., 1997, Stretching lineations in transpressional shear zones: An example from the Sierra Nevada Batholith, California: Journal of Structural Geology, v. 19, p. 29–39, https://doi.org/10.1016/S0191-8141(96)00056-9.

Tikoff, B., Davis, M.R., Teyssier, C., de Saint Blanquat, M., Habert, G., and Morgan, S., 2005, Fabric studies within the Cascade Lake shear zone, Sierra Nevada, California: Tectonophysics, v. 400, p. 209–226, https://doi.org/10.1016/j.tecto.2005.03.003.

Tikoff, B., Housen, B.A., Maxson, J.A., Nelson, E.M., Trevino, S., and Shipley, T.F., 2023, Hit-and-run model for Cretaceous–Paleogene tectonism along the western margin of Laurentia, *in* Whitmeyer, S.J., Williams, M.L., Kellett, D.A., and Tikoff, B., eds., Laurentia: Turning Points in the Evolution of a Continent: Geological Society of America Memoir 220, p. 659–705, https://doi.org/10.1130/2022.1220(32).

Tobisch, O.T., Saleeby, J.B., and Fiske, R.S., 1986, Structural history of continental volcanic arc rocks, eastern Sierra Nevada, California: A case for extensional tectonics: Tectonics, v. 5, p. 65–94, https://doi.org/10.1029/TC005i001p00065.

Tobisch, O.T., Saleeby, J.B., Renne, P.R., McNulty, B.A., and Tong, W., 1995, Variations in deformation fields during development of a large-volume magmatic arc, central Sierra Nevada, California: Geological Society of America Bulletin, v. 107, p. 148–168, https://doi.org/10.1130/0016-7606(1995)107<0148:VIDFDD>2.3.CO;2.

Tobisch, O.T., Fiske, R.S., Saleeby, J.B., Holt, E., and Sorensen, S.S., 2000, Steep tilting of metavolcanic rocks by multiple mechanisms, central Sierra Nevada, California: Geological Society of America Bulletin, v. 112, p. 1043–1058, https://doi.org/10.1130/0016-7606(2000)112<1043:STOMRB>2.0.CO;2.

Torres Andrade, E.T., and Tikoff, B., 2022, Triclinic deformation in the Courtright-Wishon shear zone, Sierra Nevada batholith, CA: Evidence for mid-Cretaceous, intra-arc magmatism in the North American Cordillera: Geological Society of America Abstracts with Programs, v. 54, no. 5, https://doi.org/10.1130/abs/2022AM-379923.

Trevino, S.F., and Tikoff, B., 2023, Two phases of Cretaceous dextral shearing recorded in the plutonic rocks of NW Nevada (USA): A tectonic link between intra-arc shearing in the Sierra Nevada and Idaho batholiths: Geosphere, v. 19, p. 1539–1564, https://doi.org/10.1130/GES02682.1.

Turner, H.W., 1894, The rocks of the Sierra Nevada: U.S. Geological Survey Fourteenth Annual Report 1892–93, Part 2, p. 435–495.

Van Auken, C., and Greene, D.C., 2013, Strain analysis and strain profile of the Mineral King pendant, southern Sierra Nevada, California: Geological Society of America Abstracts with Programs, v. 45, no. 7, p. 611.

Worm, T.J., and Greene, D.C., 2016, Syntectonic emplacement of the White Chief pluton, Mineral King pendant, Sierra Nevada, California: Implications for Early Cretaceous deformation: Geological Society of America Abstracts with Programs, v. 48, no. 7, https://doi.org/10.1130/abs/2016AM-278861.

Wyld, S.J., and Wright, J.I., 2001, New evidence for Cretaceous strike-slip faulting in the United States Cordillera and implications for terrane-displacement, deformation patterns, and plutonism: American Journal of Science, v. 301, p. 150–181, https://doi.org/10.2475/ajs.301.2.150.

Downloaded from http://pubs.geoscienceworld.org/gsa/geosphere/article-pdf/20/4/1190/6584248/ges02748.1.pdf
by guest